NKS-460
ISBN 978-87-7893-553-3

Corrosion of copper in sulphide containing environment: the role and properties of sulphide films – Annual report 2021

Elisa Isotahdon[1]

Vilma Ratia[1]

Elina Huttunen-Saarivirta[1]

Xiaoqi Yue[2]

Jinshan Pan[2]

[1]VTT Technical Research Centre of Finland Ltd., Espoo, Finland

[2]KTH Royal Institute of Technology, Stockholm, Sweden

June 2022

Abstract

In NKS-R COCOS project, the role and properties of sulphide films on copper surface were studied. This is the third annual and final report of the project.

OFP-copper samples were exposed to sulfide-containing (0-640 mg/L) anoxic simulated groundwater for different durations between 2 to 9 months. A pre-oxidation procedure was used to simulate the effect of oxic period of repository to copper surface. The corrosion behaviour was studied using mass loss determination, electrochemical measurements and several modern material characterisation methods after the exposure. In addition to sulphide concentration the chemistry of test solution was varied by additions of chloride and hydrogen carbonate. Specimens and surface deposits were studied with electron microscopy (SEM+EDS, EBSD). In-depth characterisation was done using GD-OES analysis, HE-XRD techniques and SIMS analysis. During the project, also several other analysis methods were used.

The measurable corrosion was not proportional to sulphide concentration. The corrosion was not always uniform. The corrosion rates were 0-12.3 µm/a, depending on the sulphide concentration, temperature and other variables of the environment.

EBSD results suggested that both the pre-oxidation treatment and the exposure to sulphide environment introduced the strain localization in the near-surface areas of samples. HE-XRD results showed significant heterogeneous structure deformation in the copper lattice after the exposure to test environment, both in the near surface region and deep inside the microstructure.

The sulphide-copper interactions and formation of sulphide film on copper surface were found complex processes. In this project, the world-class analytical techniques were used to investigate the penetration of chemical species into the copper microstructure. More work is needed to define the role of these chemical species as well as the nature and chemistry of the surface films that develop on copper surfaces in repository conditions.

Key words

corrosion, copper, nuclear waste, sulphide

NKS-460
ISBN 978-87-7893-553-3
Electronic report, June 2022

NKS Secretariat
P.O. Box 49
DK - 4000 Roskilde, Denmark
Phone +45 4677 4041
www.nks.org
e-mail nks@nks.org

Corrosion of copper in sulphide containing environment: the role and properties of sulphide films – Annual report 2021

Final Report from the NKS-R COCOS (Contract: AFT/NKS-R(21)127/2)

Elisa Isotahdon[1], Vilma Ratia[1], Elina Huttunen-Saarivirta[1], Xiaoqi Yue[2], Jinshan Pan[2]

[1]VTT Technical Research Centre of Finland Ltd., Espoo, Finland
[2]KTH Royal Institute of Technology, Stockholm, Sweden

Table of contents

1. Introduction 1
2. Scope of the project 2
3. Materials and methods 3
    3.1 Materials 3
    3.2 Exposure conditions 3
    3.3 Methods for corrosion monitoring 6
    3.3.1 Electrochemical methods 6
    3.3.2 Mass loss determination 6
    3.4 Characterization of materials and solutions 7
    3.4.1 Microscopy 7
    3.4.2 Water chemistry analyses 7
    3.4.3 Synchrotron Grazing Incidence X-ray diffraction (GIXRD) measurements 7
    3.4.4 Synchrotron High-Energy X-ray Diffraction (HEXRD) measurements 8
    3.4.5 Time-of-Flight Secondary Ion Mass Spectroscopy (ToF-SIMS) measurements. ... 8
    3.4.6 Glow Discharge Optical Emission Spectrometry (GDOES) 8
4. Results 9
    4.1 Corrosion measurements 9
    4.1.1 Electrochemical measurements 9
    4.1.2 Corrosion rate based on mass loss 12
    4.1.3 Visual observation of mass loss specimens 14
    4.2 Analysis of test solutions 17
    4.3 Surface characterisation with SEM 19
    4.3.1 General observations 19
    4.3.2 Observations from COCOS 2 23
    4.3.3 Observations from COCOS 3 25
    4.3.4 Generalised observations made through comparisons between samples exposed to environments across COCOS2 and COCOS3 25
    4.4 EBSD for cross-sectional samples (COCOS2) 26
    4.5 GDOES 30
    4.6 Synchrotron GIXRD results 34
    4.7 Synchrotron HEXRD results 34
    4.8 ToF-SIMS results 34
5. Discussion 36
6. Conclusions 38
7. References 39

1. Introduction

This is the final and third yearly report for the NKS-R-COCOS project entitled as "Corrosion of copper in sulphide containing environment: the role and properties of sulphide films".

The nuclear waste disposal concept in Finland and Sweden is based on a multi-barrier system (King et al., 2013), (Salonen et al., 2021). The spent nuclear fuel will be placed in cast iron containers, which are sealed inside of copper canisters. Copper canisters are further positioned in the holes drilled into deep bedrock. Canisters are surrounded by a compacted bentonite clay layer that forms a buffer around copper canisters. Bentonite buffer is believed to provide a favorable environment, where the integrity of copper canisters should be retained for at least 100 000 years. The repository conditions are believed to transform from oxic to anoxic rapidly after closure of the repository (*Nuclear Waste State of the Art Report 2011*, 2011).

Copper was chosen to serve as a corrosion barrier for the disposal canister because of its assumed resistance to corrosion under anoxic conditions. The disposal canister plays a major role in the multi-barrier concept. Possible failure mechanisms endangering the reliability of the copper canister have been assessed by models based on literature, corrosion tests simulating the disposal conditions, and copper items found in nature (King et al., 2012).

The most severe failure mechanisms of the copper canisters have been evaluated and copper-sulphide interactions have been identified as one of the possible failure mechanisms (Huttunen-Saarivirta et al., 2018; Salonen et al., 2021). Bentonite buffer might be the source of sulphide, but most importantly sulphide is expected to be formed from sulphate via microbial processes called sulphate reduction (Huttunen-Saarivirta et al., 2017). Sulphate is abundant in ground water at the disposal site, and it can also be released through cation exchange mechanisms from the bentonite buffer. Bacteria capable of reducing sulphate to sulphide are native to the groundwater at the repository site (Huttunen-Saarivirta et al., 2017). Sulphide can cause failure of copper canisters by inducing general corrosion of copper (Salonen et al., 2021). Moreover, uniform copper sulphide, Cu_2S, film could protect the canister from corrosion in certain conditions. In the event of formation of protective Cu_2S film, it is possible that the localized rupture of protective film could induce localized corrosion (Huttunen-Saarivirta et al., 2018). Indeed, the complex role and behaviour of the sulphide film on copper surfaces motivates the detailed studies on this subject.

The aim of the COCOS project was to characterise the role and properties of sulphide films on copper corrosion. The work in this project is done in collaboration between VTT Technical Research Centre of Finland Ltd, Finland, and KTH Royal Institute of Technology, Sweden. Previously published annual reports, NKS-434 (Ratia et al., 2020) and NKS-447 (Isotahdon et al., 2021), summarized the research background and description of materials, methods and results obtained in years 2019 and 2020, respectively. The report NKS-434 also contained a review section regarding the studied phenomena. A short summary of the scope of this project is given in Chapter 2. The main focus of this report is to describe the work done in the third year of the project, 2021, and summarize the main findings of the whole project period.

2. Scope of the project

Corrosion of copper under oxic and anoxic conditions, and microbiologically-influenced corrosion of copper, have been intensively investigated over the last 40 years. A recent review gives an overview of the corrosion issues, debated questions, and ongoing research programs in different countries (Hall et al., 2021). A number of SKB (Svensk Kärnbränslehantering AB) reports assessing the corrosion of copper canister under expected repository conditions have concluded that there is no considerable risk for canister failure. However, the risks for several complex forms of copper corrosion have been debated in Sweden, even in the Land and Environmental Court, leading to the statement to the Swedish Government, that supplementary information related to the long-term behaviour of the copper canisters should be presented and evaluated regarding five issues: i) corrosion due to reaction in oxygen-free water; ii) pitting due to reaction with sulphide; iii) stress corrosion cracking due to reaction with sulphide; iv) hydrogen embrittlement; v) the effect of radioactive radiation on pitting, stress corrosion cracking and hydrogen embrittlement. SKB submitted a complementary report to address these issues (SKB, 2019), however, the debate continues and is even intensified in Sweden. Earlier in 2022, the Swedish government made a decision allowing SKB to start the long process preparing for the final disposal, meanwhile requesting regular revisions of the safety risk of the system and eventual improvement. Clearly, there is a need to gain a deep understanding of the role of sulphur species and hydrogen in the embrittlement and stress corrosion cracking of copper during exposure to the ground water containing sulphide.

The aim of our work is to gain such knowledge by the detailed analyses of copper samples during and after the exposure to anoxic simulated groundwater containing sulphide. In addition to the use of traditional methods for measuring the average corrosion rate and characterization of the corrosion products formed on the copper surface, we have also utilized world-class, state-of-the-art analytical techniques to investigate the penetration of chemical species into the copper material to elucidate the reaction mechanisms.

3. Materials and methods

3.1 Materials

Hot-rolled oxygen-free phosphorus-containing copper (OFP-Cu) was used as the material for the experiments. OFP-Cu was provided by Posiva Oyj for research purposes. Two initial conditions were used in the first two long experiments (COCOS1 and COCOS2): (*i*) the polished copper surface, and (*ii*) pre-oxidised copper surface that was after grinding exposed to air at the temperature of 90 °C for seven days. The pre-oxidation was done to simulate the effect of initial exposure to oxic conditions on the copper material (prior to anoxic phase in disposal). In the third long experiment (COCOS3), all copper samples were in a pre-oxidised condition.

Three different types of copper samples were used in the project for different purposes. The electrochemical samples had the exposed area of 1 cm^2. These samples had the surface finish produced by wet grinding down to 600 grit, and were tested in as-ground (COCOS1) and pre-oxidised (COCOS2 and COCOS3) conditions. For the mass loss measurements, coupons of approximately 70 × 25 × (3-5) mm with surface finish produced by wet-grinding down to 600 grit were used. For the characterisation of corrosion products, samples with the dimensions of approximately 10 ×10 × (2-5) mm with one side of the surface further polished down to 1 µm finish were used. All samples were cleaned in acetone and ethanol prior to the test.

3.2 Exposure conditions

All exposure experiments were conducted at VTT. The samples were exposed to simulated groundwater with different levels of sulphide (S^{2-}), chloride (Cl^-) and hydrogen carbonate (HCO_3^-) additions. The chemistry (Table 1) of the simulated groundwater was derived based on modelling the groundwater chemistry of the planned disposal site with bentonite. The sulphide addition to the simulated ground water was made in the form of Na_2S. All the used sulphide additions in this project are shown in Table 2. The highest supplemented amount, 640 mg/L, was used only in the first experiment, COCOS1, initiated in 2019. The experiments were conducted at room temperature (22 °C) in a glass vessel, or at 60 °C in glass vessels placed in a heat chamber (COCOS3). The main test vessels for gravimetric samples and characterisation samples were gas-tight laboratory glass bottles with the volume of 5 L. The electrochemical samples were placed in their own bottles with the volume of 2 L. All the experiments were carried out in anoxic environment: water and vessels were flushed with argon before the start of the test. Vessels were sealed with butyl rubber stoppers to prevent oxygen contamination during the experiment. Further, vessels with electrochemical measurement setup were purged regularly with argon during the exposure period to maintain anoxic conditions.

Table 1. The chemistry of the simulated groundwater.

	K	Ca	Cl	Na*	SO_4	Br	HCO_3	Mg	Sr	Si	B	F	Mn	PO_4	lactate
mg/L	54.7	280.0	5274.0	3180.2	595.0	42.3	13.7	100.0	8.8	3.1	1.1	0.8	0.2	0.1	1

*Original Na content; actual amount is dependent on the addition of Na_2S.

Table 2. Used sulphide additions and their corresponding molar concentrations.

Sulphide (S^{2-}) addition	Concentration of the solution
0 mg/L	0
3 mg/L	10^{-4} mol/L
32 mg/L	10^{-3} mol/L
320 mg/L	10^{-2} mol/L
640 mg/L	$2*10^{-2}$ mol/L

In 2019, COCOS1 tests with the durations of about two months (53 days, 32 mg/L S^{2-}) and four months (135 days with 0, 3, 32, 320 and 640 mg/L S^{2-}) were completed. Test vessels with electrochemical measurements were initiated in 2019 and finished in early 2020, with the duration of 8 months (256 days with 0, 32 and 320 mg/L S^{2-}).

In year 2020, a 9-month long experiment COCOS2 was started with supplementary sulphide concentrations ranging from 0 to 32 mg/L. Due to the oxygen leakage in electrochemical measurements initiated in 2019, some parallel measurements were initiated in 2020 with an improved setup to reduce the possibility for air and O_2 permeation into the test vessels. The 9-month experiments started in 2020 and were terminated in the spring of 2021.

COCOS3 experiment was performed in 2021 and had the duration of four months. The sulphide level used in the test bottles was 32 mg/L and all samples were pre-oxidized. Differences between the test vessels were in further chloride and hydrogen carbonate additions to the simulated groundwater, as well as varying the test temperature so that the majority of tests were done at the temperature of 20 ºC but some of the vessels were stored at 60 °C to investigate the temperature effect.

One of the goals of this project was to study the influence of selected ions on the corrosion of copper in sulphide-containing environment. The simulated water (Table 1) had the basic level of chloride Cl^- (5274 mg/L that corresponds to 0.149 mol/L) and hydrogen carbonate HCO_3^- (13.7 mg/L that corresponds to 0.0002 mol/L). The amount of these ions was adjusted in COCOS3 by adding supplementary Cl^- (total 0.42 mol/L), in test bottles C3-ref1, C3-ref2, C3-1, C3-3, C3-NB and C3-5). In the case of test bottle C3-2, HCO_3^- was added so that the total concentration of 0.0007 mol/L was reached. In C3-3, the total HCO_3^- content was 0.0006 mol/L so that the Cl: HCO_3^- ratio was kept equal to that in the simulated water.

Smaller test vessels for the reference samples were used, two without sulphide but with chloride additions and one with added bentonite slurry. These references test bottles had the volume of 1 L, and they served only for the characterization samples.

Table 3. Summary of the test series during the project. Colours indicate the different sulphide concentrations.

			Sample types with ground surface			Sample types with pre-oxidation			
Name of experiment (year) and test bottles	Solution: Simulated water + X mg/l S, + addition of Cl or HCO_3	Duration months	Electrochemical	Gravimetry	Characterisation	Electrochemical	Gravimetry	Characterisation	**Temperature, °C**
C O C O S 1 (2019)									
C1-1, 0mg	Simulated water only	4	1*	1	1		1	1	20
C1-2, 3.2 mg	3 mg/l S	4			1			1	20
C1-3, 32mg	32 mg/l S	4	1*	1	1		1	1	20
C1-3_B, 32mg	32 mg/l S	2			1			1	20
C1-4, 320mg	320 mg/l S	4	1	1	1		1	1	20
C1-5, 640mg	640 mg/l S	4			1			1	20
C O C O S 2 (2020-2021)									
C2-1, 0mg	Simulated water only	9		1	1		1	1	20
C2-2, 3.2 mg	3.2 mg/l S	9		1	1	1**	1	1	20
C2-3, 32mg	32 mg/l S	9		1	1	1	1	1	20
C2-4, 320mg	320 mg/l S	9		1	1		1	1	20
C O C O S 3 (2021)									
C3-ref1, 0 mg/L + Cl	Cl	4						1	20
C3-ref2,0 mg/L + Cl	Cl	4						1	60
C3-1, 32 mg/L + Cl	32 mg/L + Cl	4				1	1	1	20
C3-2, 32 mg/L + HCO3	32 mg/L + HCO_3	4				1	1	1	20
C3-3, 32 mg/L +Cl + HCO3	32 mg/L +Cl + HCO_3	4				1**	1	1	20
C3-NB, 32 mg/L + Cl+ bentonite	32 mg/L + Cl+ bentonite	4						1	20
C3-4, 32 mg/L	32 mg/L	4					1	1	60
C3-5, 32 mg/L + Cl	32 mg/L + Cl	4					1	1	60

*) oxygen leakage during the test, **) small amount of oxygen was found in the solution after the test, yet no oxygen leakage was detected during the test. Additionally, in all the 60°C tests, small amount of oxygen was detected with a microelectrode; this is likely due to decrease in the solubility of oxygen in water with increase in temperature

3.3 Methods for corrosion monitoring

3.3.1 Electrochemical methods

The corrosion behaviour of the samples was monitored with electrochemical measurements. Open circuit potential (OCP) and redox potential data were collected continuously throughout the experimental period. The used reference electrode was Ag/AgCl (anaerobic, 0.15 M KCl). A platinum electrode immersed in the vessels was used for redox measurements.

Linear polarization resistance (LPR), electrochemical impedance spectroscopy (EIS) and Tafel measurements were conducted once a week. Counter electrode was platinum, and the copper sample was used as a working electrode and another similar copper sample as a pseudo-reference electrode in the measurements. Potential range in LPR measurements was -20 to 20 mV vs. E_{OC} with the scan rate of 0.16667 mV/s, while that in Tafel measurements was from -30 to 30 mV vs. E_{OC} with the scan rate of 0.16667 mV/s. Tafel measurements were performed over a more narrow potential range than usually, in order to avoid the perturbation of the system; such approach has proved successful in earlier studies. The EIS was measured at OCP with 10 mV AC voltage, from 100000 to 0.001 Hz, eight points per decade. The OCP measurements were conducted for 60 s at the start of these measurements. All the electrochemical measurements were performed using a Gamry Instruments potentiostat model Reference 600™ with DC105 and EIS300 software. Gamry Echem software was used to fit the Tafel and polarisation resistance plots.

The corrosion rate was calculated from the corrosion current in two different ways. The calculation of the corrosion rate (CR) is derived from the Faraday's law. According to ASTM standard G102-89 it is calculated as:

$$CR = (i_{corr} * K * EW)/\rho$$

where i_{corr} is corrosion current density (corrosion current I_{corr} divided by the exposed sample area), K is a constant depending on the wanted unit of the outcome, EW equivalent weight and ρ the density of copper. For corrosion rates presented in mm/a, the constant K is 3272 mm/(A*cm*year).

In the first method, the I_{corr} is determined by using Tafel extrapolation. In the second calculation method, I_{corr} is calculated with the formula:

$$I_{corr} = (\beta a * \beta c)/(2.303 * Rp * (\beta a + \beta c))$$

where the β coefficients are obtained from the Tafel plots and the polarisation resistance (Rp) from the linear polarisation curve.

3.3.2 Mass loss determination

Mass losses were determined for most of the samples exposed to the different environments. After the exposure, corrosion products on sample surface were removed by pickling solution containing 500 mL of HCl (37%), 500 mL distilled water and 3.5 g of hexamethylenetetramine ($(CH_2)_6N_4$). The pickling was done 3-5 times, until a steady weight was achieved for the sample.

Based on this mass loss, the corrosion rate (r_{corr} in µm/a) was calculated with the formula:

$$r_{corr} = (d\mathit{m} \cdot 365 \cdot 10)/(\mathit{A} \cdot \mathit{t} \cdot \rho)$$

where d*m* is mass loss (mg), A area (cm^2), t time (d) and (ρ) density of copper (g/cm^3). The mass loss results, based on which the calculations were made, were corrected for the pickling with reference samples: similar samples in untreated and pre-oxidised state was pickled and

mass loss from the pickling in comparison to the original untreated mass was retracted from the results to eliminate the effects of pickling.

3.4 Characterization of materials and solutions

Several different characterization methods were applied in COCOS project to examine the samples and their test environment. The methods that were found suitable and used in last year of project are described in this chapter. The other used methods are described in previous annual reports of the project.

3.4.1 Microscopy

To study the grain size and orientation of the test material, one sample was etched with the same pickling solution as used in mass loss determination (H_2O + HCl + $(CH_2)_6N_4$) and then studied with an optical microscope Leica MZ7.5.

All samples were visually inspected and photographed after the exposure. The surfaces were also examined with an optical stereomicroscope Leica MZ7.5. Scanning electron microscopes with field emission gun (FEGSEM) Zeiss UltraPlus Gemini and Zeiss UltraPlus Merlin were used for characterising in more detail the surface morphologies in secondary electron (SE) and backscattered electron (BSE) modes after the exposure. Moreover, energy dispersive X-ray spectroscopy (EDS) with Thermoscientific UltraDry spectrometer was used to obtain information on the chemical composition of the surfaces. The Electron Backscatter Diffraction (EBSD) detector attached to FEGSEM was also employed for investigating the crystallography of selected samples in cross section. Samples for EBSD measurements were prepared using Buehler VibroMet 2 vibratory polisher for 12-18 hours to remove remaining deformation after mechanical sample preparation. EBSD analyses were conducted using the acceleration voltage of 20 kV and the working distance of 8-9 mm with the tilting stage. EBSD data were presented as inverse pole figures (IPF), local average misorientation (LAM) maps with grain boundaries (GB), and grain average misorientation (GAM) maps.

3.4.2 Water chemistry analyses

The water chemistry analyses were conducted for water samples collected from each test vessel after the exposure tests (COCOS1, COCOS2, COCOS3) by ALS Finland Oy with a number of methods. pH, alkalinity, conductivity, acidity, carbon dioxide and carbonates were determined with potentiometric titration (EN ISO 9963-1 and CSN 75 7373); Br, F, Cl and SO_4 with ion chromatography (ISO 10304-1, EN 16192); hydrogen sulphide (HS^-) and sulphide (S^{2-}) with spectrophotometry (CSN 83 0520-16, CSN 83 0530-31, SM 4500-S D); and B, Ca, Cu, Mg, Mn, K, Na, Si, Sr with inductively coupled plasma - mass spectrometry and atomic fluorescence spectroscopy (EPA 200.8, EN ISO 17294-2, EPA 6020A, EPA 245.7, EPA 1631, EN ISO 178 52, EN 16192).

3.4.3 Synchrotron Grazing Incidence X-ray Diffraction (GIXRD) measurements

In January 2020, the KTH group performed synchrotron GIXRD measurements of the 4-month samples (COCOS1) using the surface diffraction beamline I07 at Diamond Light Source in the UK. The diffracted signal was measured with an incidence angle of 0.2° and 0.05°, respectively. The energy of the incident X-ray beam was 20.5 keV, with a beam size of 100 µm (vertical) x 300 µm (horizontal) at the sample position. The experiment was performed with a DECTRIS Pilatus 100K two-dimensional detector at a distance of 900 mm from the sample. The high flux of the beam and the grazing incidence angles in the XRD experiments allowed a high surface sensitive in the detection of the thin layer of corrosion products, and also probing of the

outermost surface grains to measure the evolution of lattice strain associated with hydrogen infusion.

3.4.4 Synchrotron High-energy X-ray diffraction (HEXRD) measurements

In August 2019, the KTH group performed the first HEXRD measurements of three 2-month samples (COCOS1) at the Swedish Materials Science beamline P21.2 at PETRA III in DESY, Hamburg, Germany. The photon energy used was 96 keV and the distance between the sample and the Varex 4343CT flat panel detector was about 1.6 m. The sample surface was aligned to be parallel to the X-ray beam which was 20 μm (vertical) x 55 μm (horizontal). The entire specimen was scanned in 20 μm steps across the specimen thickness. The 2D diffraction images were converted into 1D patterns by integrating the diffraction data along all azimuthal angles. The HEXRD signals were measured in transmission mode while the sample was scanned from the surface down to the bulk, so the diffraction data provide the information of the lattice deformation in the microstructure. In the summer of 2021, the second HEXRD measurement was performed on four 9-months samples (COCOS2) using the same setup as in the first measurement, via remote way (samples sent to DESY) due to Covid-restrictions. Moreover, in March 2022 we perform the HEXRD measurement again of the four 9-month samples (COCOS2) using a new setup to increase the grain statistics.

3.4.5 Time-of-Flight Secondary Ion Mass Spectroscopy (ToF-SIMS) measurements.

In order to investigate the penetration and distribution of the chemical species that might contribute to the degradation of copper, particularly S, Cl, O and H, the KTH group performed ToF-SIMS measurements for the copper samples including four 2-month samples (COCOS1), four 9-month samples (COCOS2), and three new 4-month samples (COCOS3). The measurements were performed at the Infrastructure for Chemical imaging at Chalmers University of Technology, using a ToF-SIMS V instrument (ION-ToF, GmbH, Münster, Germany) equipped with a 25 keV Bismuth LMIG (Liquid metal ion gun) and a 10 keV Cs sputter gun providing high precision information on the concentration of the elements, with a mass resolution m/Δm: 6000, and focus of the ion beam: 1–2 μm. Both image and depth profile analyses were performed using the ION-ToF Surface Lab software (Version 6.3, ION-ToF, GmbH, Münster, Germany).

3.4.6 Glow Discharge Optical Emission Spectrometry (GDOES)

Glow Discharge Optical Emission Spectrometry (GDOES) was performed as depth profile analysis of sulphur and oxygen by Spectruma Analytik, Germany. Analysis was done using GDA 750 HR instrument with 2.5 mm anode. Photomultiplier optics detection was used. Analyses were done for two COCOS2 samples that had been exposed to 32 mg/L sulphide environment. One sample with ground and one with pre-oxidised surface were analysed (sample codes C2-3-O and C2-3-N, bottle C2-3). Two spots with the diameter of 2.5 mm from both samples were analysed.

4. Results

4.1 Corrosion measurements

4.1.1 Electrochemical measurements

The OCP and redox values for the samples and the solution, respectively, were continuously monitored during all three test series. In the first year of the project, unfortunately, an oxygen leakage was detected in one test bottle (Table 3) as the solution contained significant amount of oxygen after the test, and thus, some of the results from electrochemical measurements in COCOS1 are partly questionable, and therefore some of the planned experiments were modified to avoid the oxygen leakage in COCOS2.

The second long electrochemical measurement in COCOS2 had two measurement units with the sulphide concentrations of 3.2 and 32 mg/L. The results showed that, the highest OCP and redox potential values were recorded in the environment with lower sulphide content, 3.2 mg/L (Figure 1) with the OCP value being close to 0 mV vs. Ag/AgCl at the end of measurement. Figure 1 also revealed that both OCP and redox values for the copper samples in 3.2 mg/L solution were initially at a low level, almost at the same level than in the corresponding system with 32 mg/L sulphide, but they increased radically by several hundreds mVs within the first weeks of exposure. In contrast to this, the OCP and redox potential for the sample in 32 mg/L sulphide environment were retained at much lower values and almost constant for the entire measurement period: the OCP was systematically about -850 mV vs. Ag/AgCl, while the redox was -400 mV or lower all though the test. In the previous (COCOS1) experiment, distinct increases in OCP values were detected for the sample in environment with 32 mg/L sulphide. It was speculated that the increase in OCP could be attributed to the fact that sulphide in the water had been consumed by chemical reactions that were enhanced by oxygen leakage. Similar increase in OCP for COCOS2 sample in 3.2 mg/L sulphide environments was detected after 100 days. Again, some leaked oxygen was found in 3.2 mg/L sulphide test bottle after the test (Table 3). Also, similar increase in OCP was found in earlier experiment also for environment without sulphide additions ("0 mg/L COCOS1"). It can be concluded that sudden increases in the OCP and redox potential in all three experiments in COCOS project were likely related to the partial oxidation of test solution or consumption of the added sulphide.

The OCP values of the COCOS2 and COCOS3 samples exposed to 32 mg/L sulphide with and without further chloride and hydrogen carbonate additions are presented in Figure 2. Here, all values were very stable, about -850 mV vs Ag/AgCl (note the different scale in y-axis compared to Figure 1). Slight increase in OCP, less than 50 mV, was seen during the 4-month measurement period. The difference between the curves was not significant, meaning that the addition of Cl^- of HCO_3^- did not significantly influence the open circuit potential of the sample. The measurement period was almost 9 months in COCOS2 and 4 months in COCOS3, respectively. The OCP and redox potential values stabilized in these environments within 100 days, and therefore the 4-month period was found representative.

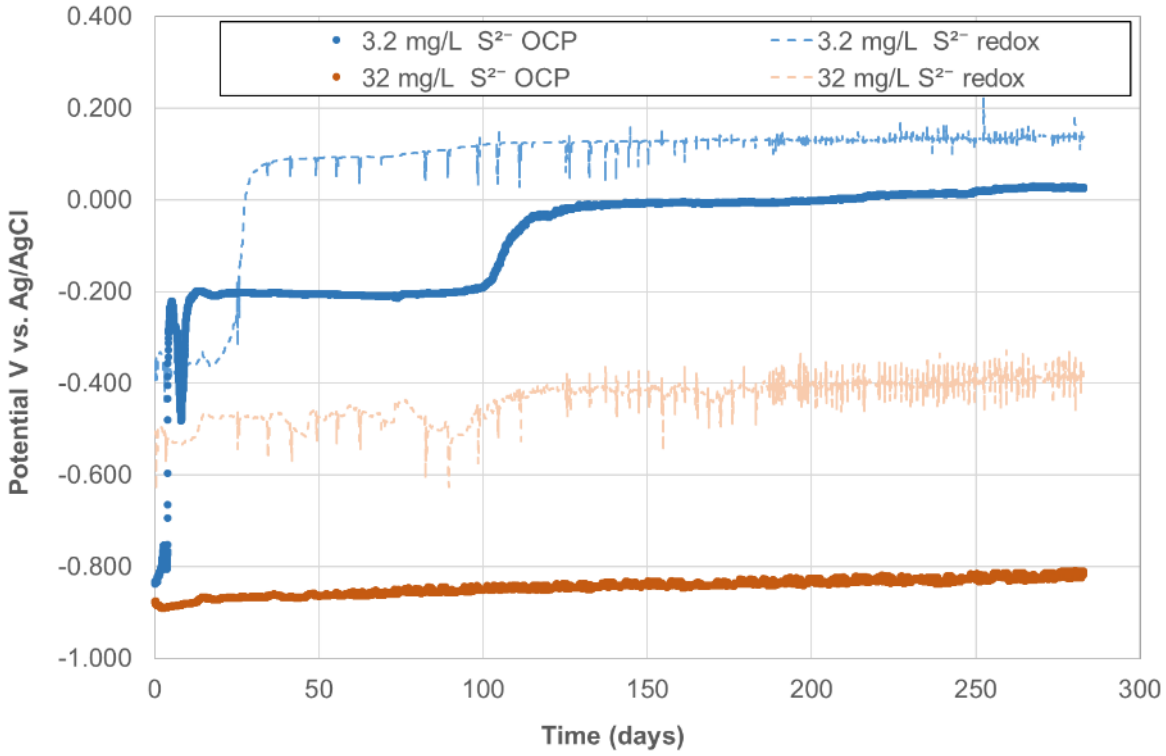


Figure 1. OCP and redox potential vs. time for specimens exposed to 3.2 and 32 mg/L sulphide, COCOS2.

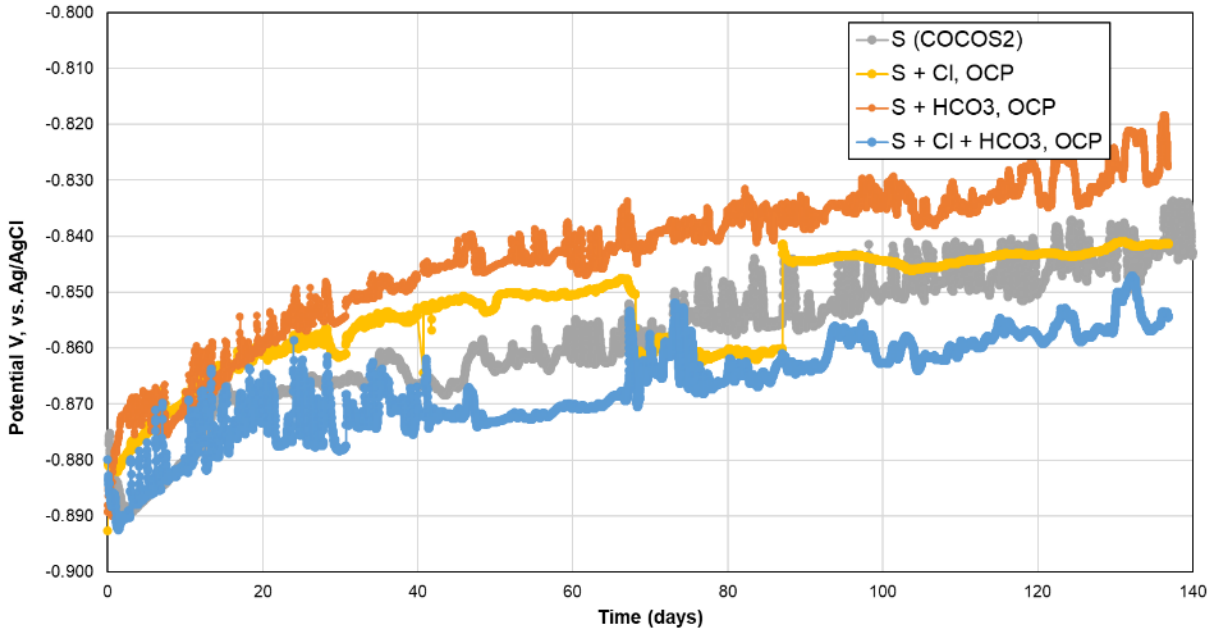


Figure 2. OCP vs time for specimens exposed to 32 mg/L sulphide with and without Cl^- and $HCO3^-$ additions, data from COCOS2 and COCOS3 tests.

The corrosion rates for the copper samples were determined based on Tafel plots and LPR measurements done intermittently during the exposure period. The corrosion rates for the samples in COCOS2 are presented in Figure 3. The calculated corrosion rates for the samples in both test bottles (3.2 and 32 mg/L sulphide) were below 5 µm/a. The corrosion rate of sample in the environment with only 3.2 mg/L sulphide was higher than that with 32 mg/L sulphide, which may be related to the possible leaked oxygen in this test bottle. However, while the OCP

for the sample exposed to simulated groundwater with 3.2 mg/L sulphide increased already within the first weeks of the test, the increase in corrosion rate occurred slightly later, after about two months (60 days). It is possible that the change in the OCP level and oxidation capacity of the environment altered the characteristics of the corrosion products, thereby also the increase in the corrosion rate. In the case of the sample exposed to simulated groundwater with 32 mg/L sulphide, the corrosion rate was slightly above 1 µm/a in the beginning of the test but soon stabilized to values below 1 µm/a. Such low corrosion rate values are typical of the passive state.

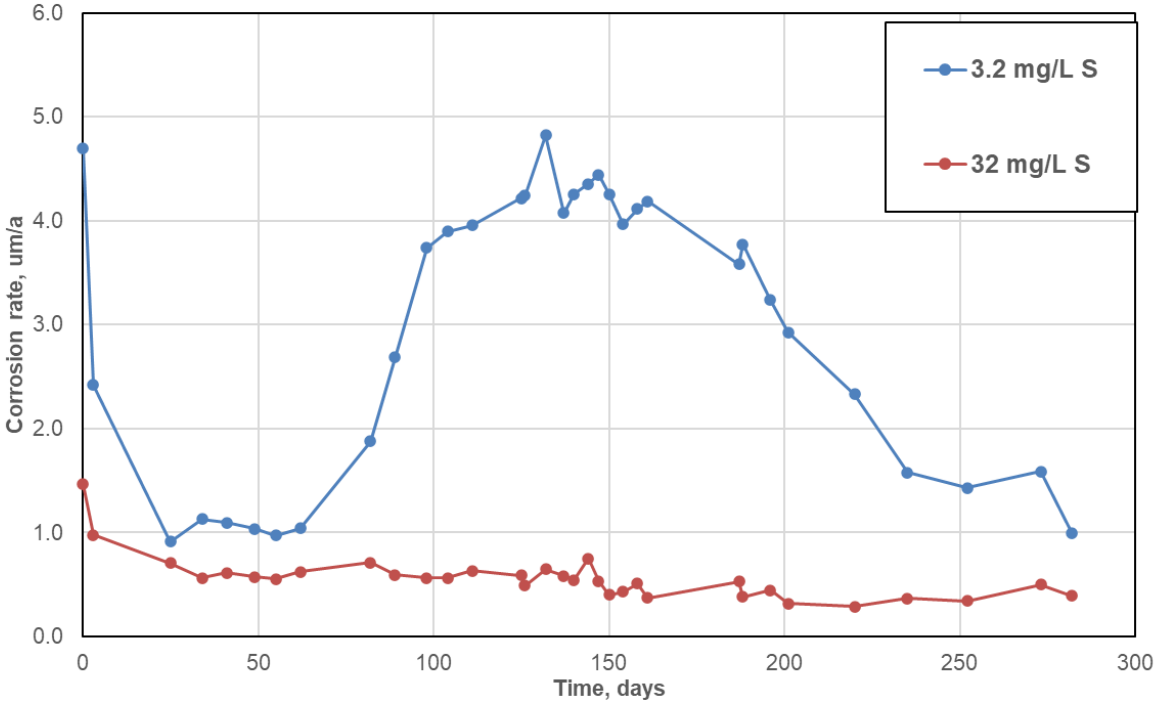


Figure 3. Corrosion rate (µm/a) calculated from Tafel plots and LPR measurements, COCOS2.

The calculated corrosion rates for COCOS3 samples that were exposed to the simulated groundwater with added Cl^- and HCO_3^- were equal to those of the samples exposed to groundwater with 32 mg/L sulphide without further additions of Cl^- and HCO_3^-. The first measurement point in the beginning of test gave momentary corrosion rates of 4 µm/a and 5 µm/a for the samples in 32 mg/L sulphide + Cl^- and 32 mg/L sulphide + HCO_3 environments, respectively. After about 30 days of immersion, all calculated corrosion rates stabilized below 1 µm/a and were retained quite constant during the rest of the measurement period. The corrosion rates in HCO_3^- containing environments were slightly lower than those without HCO_3^- addition, but the difference was minor.

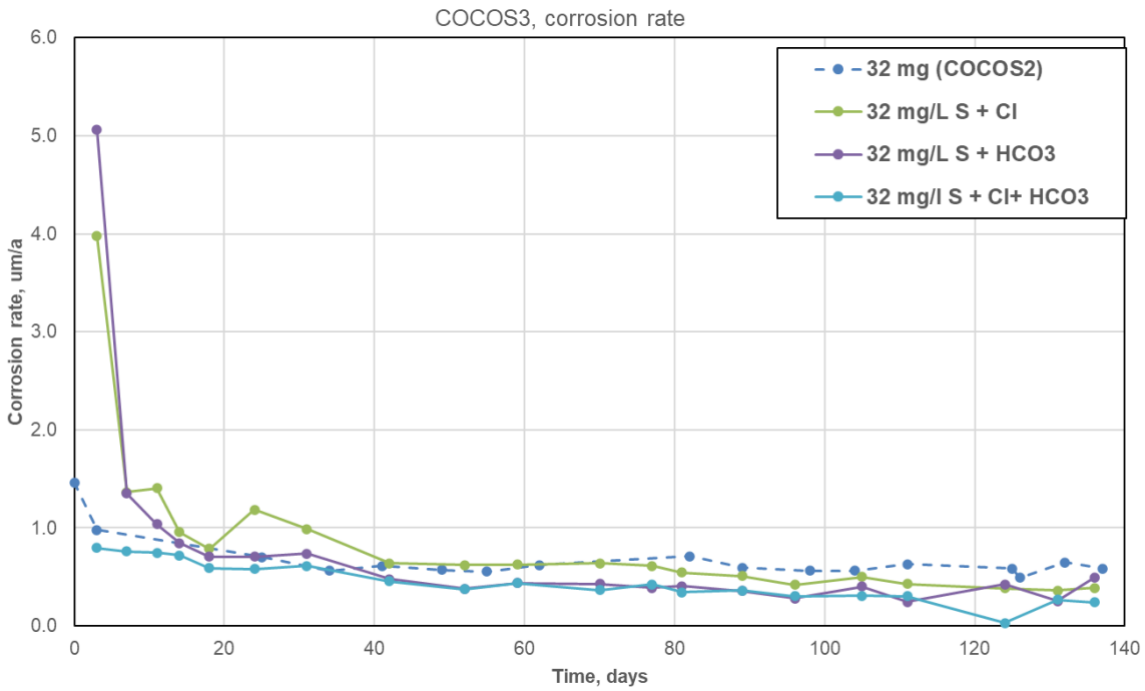


Figure 4. Corrosion rate (µm/a) calculated from Tafel plots and LPR measurements, COCOS3.

4.1.2 Corrosion rate based on mass loss

All mass loss results were converted into corrosion rates (µm/a). The corrosion rates of samples studied in COCOS1 test were already reported in previous yearly report but are shown here for comparison (Figure 5). In two of the first test series, COCOS1 and COCOS2, samples with two surface conditions were tested: pre-oxidised and non-preoxidised (ground). The trend in COCOS1 was that the pre-oxidised samples generally had higher mass losses than the ground specimens, corresponding to higher corrosion rates. All cumulative corrosion rates after the 4-month test were between 0.30 – 0.49 µm/a. The highest mass losses were found for the samples in 32 mg/L sulphide environment, although the difference to 0 and 320 mg/L sulphide environments was very small. In COCOS2 (Figure 6), the same trend with the surface finish was found, i.e., the corrosion rate of the pre-oxidized samples was higher with the exception of samples exposed to 320 mg/L sulphide. The deviation of results was quite large. However, the corrosion rates for the samples were significantly higher than in COCOS1 in environments with 3.2 mg/L and 320 mg/L sulphide: in 3.2 mg/L sulphide solution, the corrosion rates were 10.90 µm/a for ground and 11.20 µm/a for the pre-oxidized samples, while in 320 mg/L sulphide solutions the corresponding values were 12.73 µm/a and 10.10 µm/a, respectively. These values were more than tenfold in comparison to copper corrosion rates measured in other test environments of COCOS1 and COCOS2. In COCOS2, the samples exposed to simulated groundwater without sulphide additions (0 mg/L) suffered only negligible corrosion (0.01 µm/a and 0.07 µm/a). In the solution with 32 mg/L sulphide, the corrosion rates that were detected for pre-oxidized and ground samples were 0.24 µm/a and 0.29 µm/a.

Determination of corrosion rates based of mass loss is based oncumulative mass losses for the specimens over the test time. The test duration differed between the COCOS experiments so that the duration of COCOS1 was less than half of the duration of COCOS2. As the progress of corrosion is not necessarily linear in time, this may have an effect on the results. Based on the measurements on the samples exposed to different sulphide contents, no direct correlation could be found between the sulphide content of the environment and the material corrosion rate. The role of sulphide addition is complex: it is likely related to the nature and properties of the surface

films that develop during the exposure, which likely correlates with the amount of added sulphide, and duration of the test. The significant difference between the corrosion rates of samples exposed to 320 mg/L sulphide in COCOS1 and COCOS2 is probably linked with the differences in nature and properties of the surface films. Further, the method of removal of the corrosion products by pickling plus the possibility of localized corrosion may also have some influence on the results.

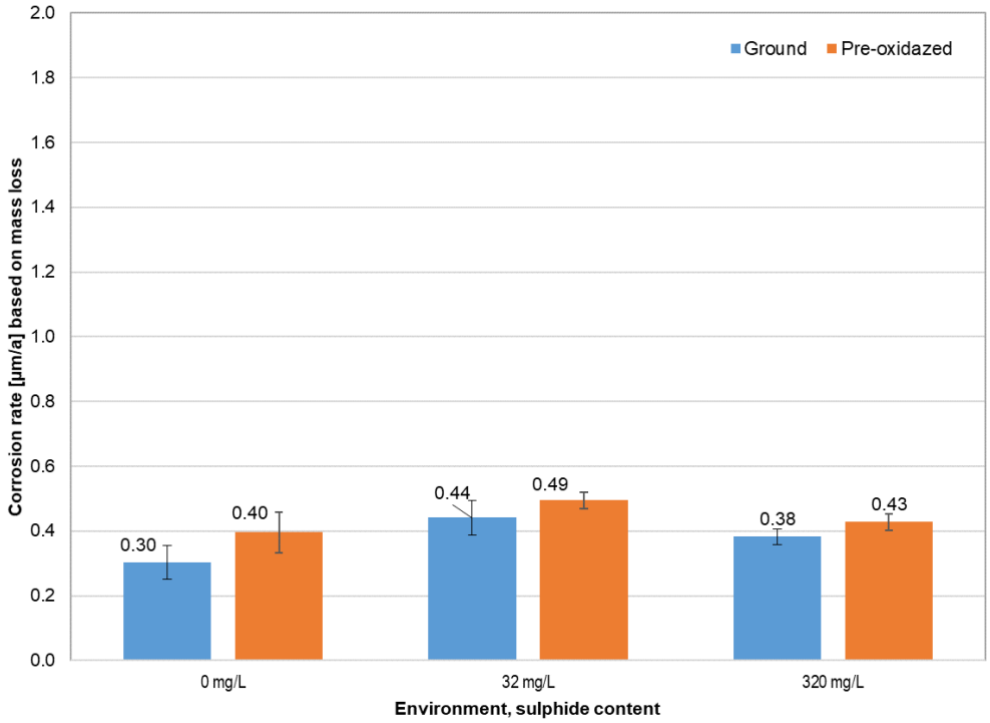


Figure 5. Corrosion rates based on cumulative mass loss obtained in COCOS1 test, 4 months test**.**

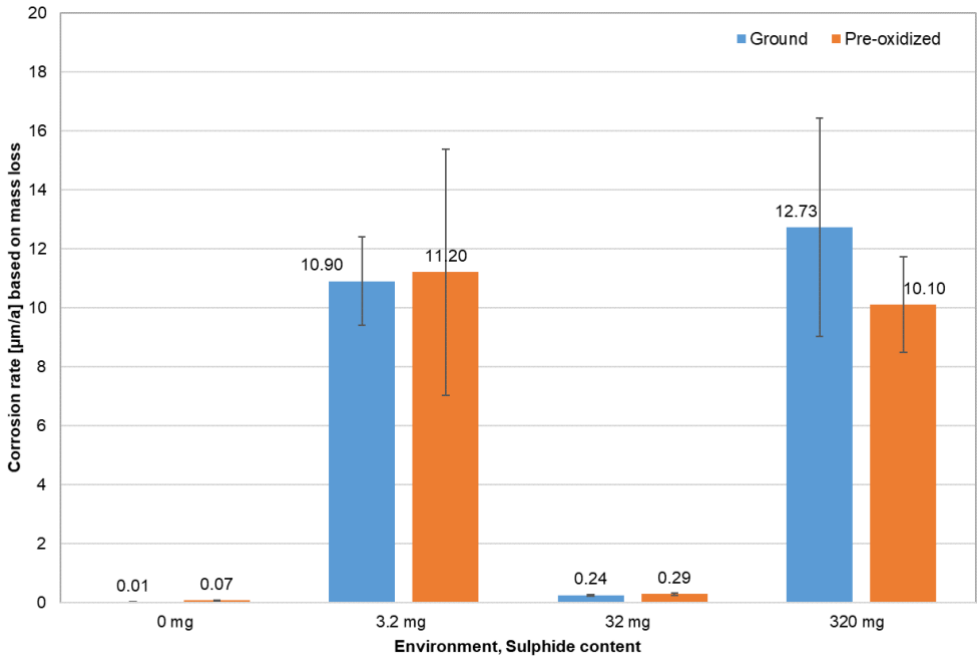


Figure 6. Corrosion rates based on cumulative mass loss obtained in COCOS2 test, 9 months test**.**

In COCOS3 test, the amount of added sulphide in all test vessels was 32 mg/L and all samples were pre-oxidized. The results obtained at room temperature with 32 mg/L sulphide and supplementary chlorides and/or carbonates showed very minor differences between the corrosivity of solutions. The copper cumulative corrosion rates were slightly lower, in the range from 0.15 to 0.22 µm/a, than the corresponding results from previous tests with 32 mg/L (0.49 and 0.29 µm/a) S^{2-}. Exposure to solutions at higher temperature (60°C) resulted in evidently higher copper corrosion rates compared to the tests at room temperature, rates being 1.36 and 1.28 µm/a.

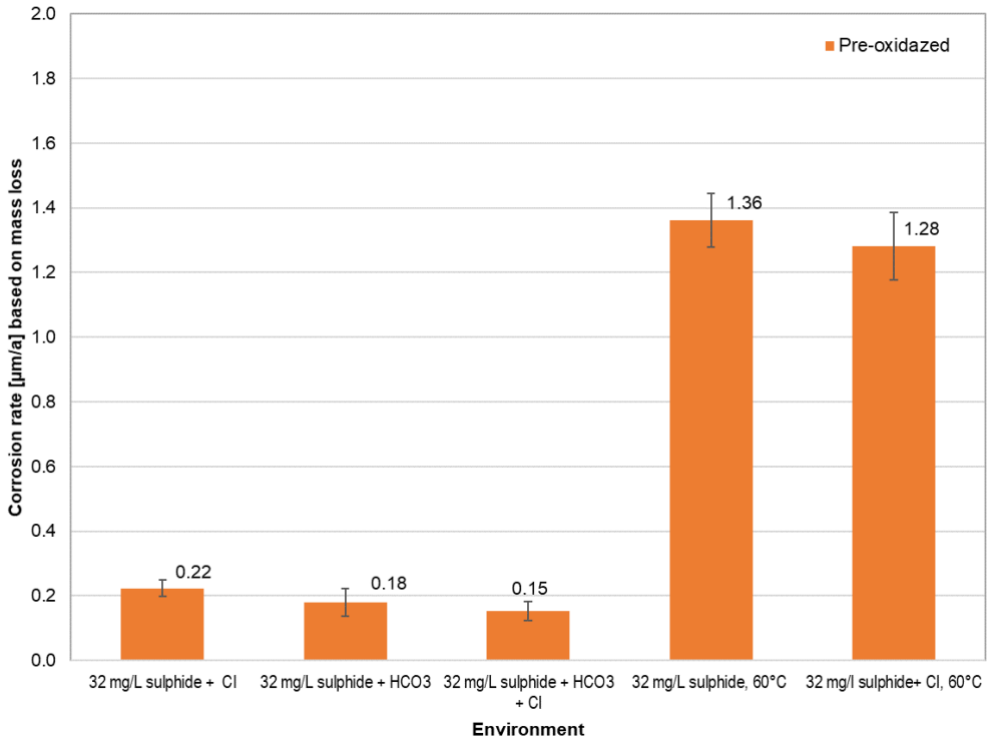


Figure 7. Corrosion rates based on cumulative mass loss obtained in COCOS3 test, 4 months test.

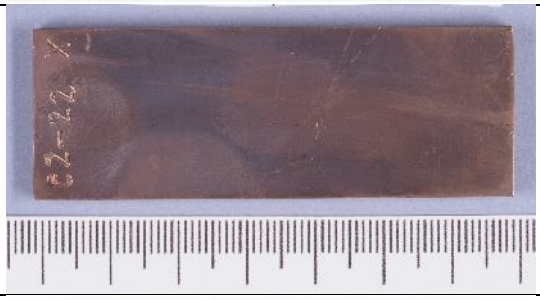
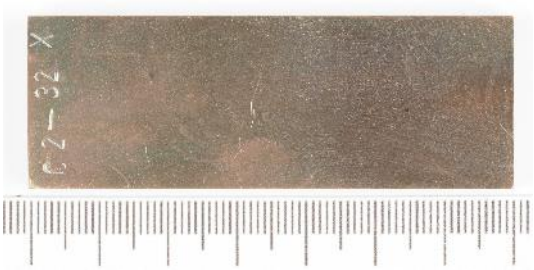
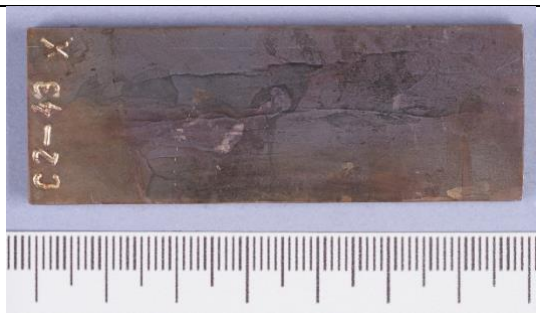
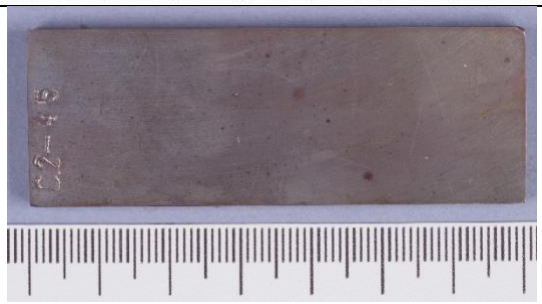
4.1.3 Visual observation of mass loss specimens

The typical surface appearance of mass loss samples, prior to etching, is shown in Table 4 for COCOS2 samples and in Table 5 for COCOS3 samples. In both tests, plenty of variation in the outlook of specimens was found in terms of colour and surface deposits visible to bare eye.

In COCOS2 when sulphide concentration was varied from 0 to 320 mg/L, differences can be found in the colour of copper surfaces after the exposure. The surface deposit becomes more evident and darker at higher sulphide concentrations. At 0 mg/L of sulphide, that is, the simulated baseline groundwater only, surfaces were still quite bright and copper reddish after the test, with only occasional areas of darker deposit being detected. Also, the negligible weight losses indicated that the surfaces were not much affected by the exposure. In the specimens exposed to 3.2 mg/L sulphide, the surface deposit was darker, and for the specimens exposed to 32 mg/L sulphide, the surface deposit was greenish in colour. The surface of samples exposed to 320 mg/L sulphide, the surface deposit was dark, similarly to those exposed to 3.2 mg/L sulphide. Therefore, it is evident that in such cases where a dark deposit developed on the sample surfaces, the weight losses after the tests were large, implying the dark deposits were relatively thicker or denser than e.g, the greenish deposit (32 mg/L). Systematic differences between the appearance of pre-oxidised and ground surface were not detected. Technical

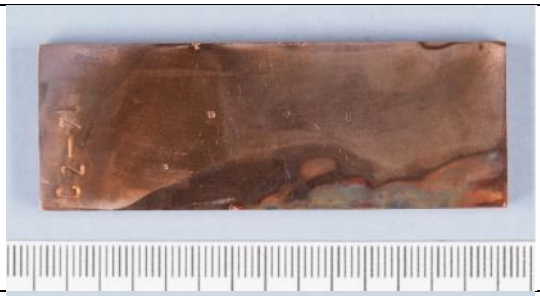
observation was that the position of samples had an effect on the sample appearance: irregular darkening of the surfaces was observed when the samples were positioned in the bottom of the test bottle, with the large face towards the glass being less corroded. Therefore, a sample holder for the COCOS3 test was developed to keep all the surfaces directly exposed to the surrounding environment. Holder was made of a plastic ring, that supported the sample in order to avoid straight contact with bottom of the glass bottle and to provide similar conditions to all faces of the sample.

Table 4. Typical surface appearance of the mass loss samples, COCOS2 test.

Test	Example surface of pre-oxidised sample	Example surface of non-pre-oxidised (ground) sample
C2-1 0 mg/L S		
C2-2 3.2 mg/L S		
C2-3 32 mg/L S		
C2-4 320 mg/L S		

In COCOS3, the surface appearance varied greatly between individual samples and sides. A clear difference in the surface appearance could be seen between the samples exposed to the solutions at room temperature and at 60°C, Table 5. The surfaces of test materials exposed to room temperature contained dark deposit that was unevenly distributed on the surfaces. The surfaces of the samples exposed at 60°C had dark greyish deposits that were more uniform than the deposits formed at lower temperatures.

Table 5. Typical surface appearance of the mass loss samples (all pre-oxidised), COCOS3 test.

Test	Example surface 1	Example surface 2
C3-1 32 mg/L S + Cl		
C3-2 32 mg/L S + HCO3		
C3-3 32 mg/L S + Cl+ HCO3		
C3-4 32 mg/L S, 60°C		
C3-5 32 mg/L S + Cl, 60°C		

Some of the mass loss coupons in COCOS3 test featured, along with the deposit formation, large black "pits" on one surface of the sample, examples from two test bottles with 32 mg/L sulphide with added chloride and carbonate are shown in Figure 8. In COCOS1 test series (in which the test specimens were located horizontally in the bottom of the test containers) it was noticed that, in some cases, the added Na_2S (solid granules) had not dissolved efficiently enough but deposited on some of the samples, causing the appearance with darker spots (Ratia et al., 2020). After COCOS1, the procedure of adding Na_2S to solution was changed from adding

Na_2S granules straight to solution to so the procedure in which the granules were first dissolved into a small volume of the test solution, which was then added into the test bottle. After this procedure, in COCOS2, similar defects were not found. In COCOS3, the black large pits were already visible after about a week of immersion, that could support the theory of incomplete dissolution of Na_2S, although the samples were not horizontally positioned in the bottle. However, the appearance was slightly different to that of samples in COCOS1 and the procedure was improved to avoid the incomplete dissolution. Also, these marks were found only mass loss coupons, not in smaller characterisation samples. Therefore, the nature of these defects cannot be explained, and they may be an artifact or part of the corrosion process, indicating the possibility of localized corrosion phenomenon.

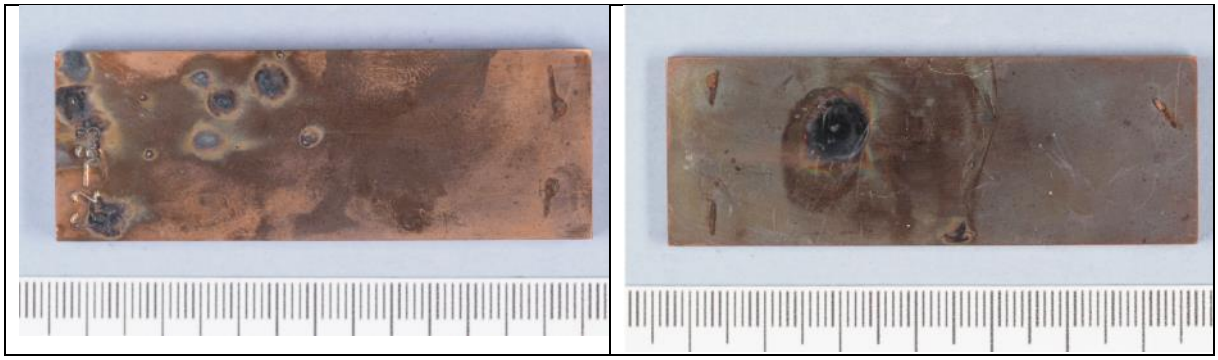


Figure 8. Examples of mass loss coupons with black marks after the COCOS3 test, a) 32 mg/L S + Cl, b) 32 mg/L S + Cl +HCO_3.

4.2 Analysis of test solutions

The water chemistry of the test solutions was analysed after the COCOS2 (Table 6) and COCOS3 (Table 7) tests, similarly to what in previously reported for COCOS1 (Ratia et al., 2020). For reference, the calculated contents in the simulated groundwater are shown in the right column of Table 7. It can be seen that Mg and Si contents decreased, and pH value of the solution slightly increased when more sulphide was added to test solution. The highest amounts of copper (total and soluble) were detected in the bottles with no sulphide addition, indicating that all the formed deposits (dark or green) gave some protection against copper dissolution**.** The detected carbonate content increased with increase in pH value of the solution, being higher with greater sulphide additions. In the solutions with 32 mg/L and 320 mg/L, the final sulphide contents were lower than the additions, indicating that some of the sulphide may have consumed upon the deposit formation.

Table 6. Water chemistries after the COCOS2 (C2) tests. On the right-hand side, also the original values of the simulated groundwater components are presented.

Component	**Unit**	C2-1 (0 mg S)	C2-2 (3.2 mg/L S)	C2-3 (32 mg/L S)	C2-4 (320 mg/L S	Simulated groundwater (calculated)
pH		7.85	8.53	8.67	10	
conductivity	mS/m	1640	1540	1660	1620	
chloride	mg/L	5250	5400	5580	5410	5274
sulphate	mg/L	604	639	507	705	595
alkalinity, pH 4.5	mmol/L	0.44	0.515	0.87	9.3	
alkalinity, pH 8.3	mmol/L	<0.150	<0.150	<0.150	1.03	
fluoride	mg/L	<1.00	<1.00	<1.00	<1.00	0.8
hydrogen sulphide	mg/L	<0.010	11.8	20.1	162	
sulphide (S2-)	mg/L	<0.010	11.1	18.9	152	0
bromide	mg/L	42.7	40.6	43.8	41.8	42.3
carbonates (CO3 2-)	mg/L	0.00	2.5	4.9	61.6	
hydrogen carbonate (HCO3-)	mg/L	26.8	26.4	43.2	442	13.7
carbon dioxide, total	mg/L	19.4	20.8	34.7	364	
Cu, all	mg/L	0.375	<0.0100	<0.0100	0.0015	
Soluble metals						
B	mg/L	1.9	1.61	2.23	3.93	1.1
Ca	mg/L	265	263	268	250	280
Cu, soluble	mg/L	0.0174	<0.0100	<0.0100	<0.0100	
K	mg/L	51.8	52.7	53.4	52.4	54.7
Mg	mg/L	94.1	91.8	99	13.4	100
Mn	mg/L	0.0914	0.0335	0.0131	<0.00100	0.2
Na	mg/L	2970	3260	3060	3530	3180
Si	mg/L	6.89	6.73	5.11	0.327	3.1
Sr	mg/L	8.97	9.13	9.25	8.94	8.8

In COCOS 3 (results presented in Table 7), the addition of HCO_3 was found to increase the pH value. In the reference bottles with chloride addition (C3-Ref1 and C3-Ref2) without sulphide addition, evidently higher copper concentrations were found, indicating that in the presence of chloride, sulphide addition provides protection for dissolution of copper. This may indicate the formation of insoluble compounds or layer in the copper surface in presence of these element.

Table 7. Water chemistries after the COCOS3 (C3) tests.

Component	Unit	C3-1, High Cl	C3-2, High HCO3	C3-3, High Cl and HCO3	C3-4, 60C	C3-5,High Cl in 60 C	C3-Ref1, No S, high Cl	C3-Ref2, No S, High CL 60C	C3-NB, S + Cl + Bentonite
pH		9.04	9.14	9.2	7.95	7.83	8.34	7.75	8.27
conductivity	mS/m	4160	1660	4150	1660	4140	4180	4120	4410
chloride	mg/L	15700	5250	15800	5240	15300	12800	15600	13100
sulphate	mg/L	607	616	588	626	608	611	614	1260
alkalinity pH 4.5	mmol/L	1.12	1.87	1.72	0.904	0.669	0.443	0.434	1.12
alkalinity pH 8.3	mmol/L	0.216	0.334	0.381	<0.150	<0.150	<0.150	<0.150	<0.150
fluoride	mg/L	<1.00	0.814	<1.00	0.507	<1.00	<1.00	<1.00	<1.00
bromide	mg/L	41.1	42.5	40.7	43.1	40.8	40.8	40.5	42.9
carbonates (CO3 2-)	mg/L	13	20.1	22.8	0.0	0.0	0.0	0.0	1.15
acidity, pH 8.3	mmol/L	<0.150	<0.150	<0.150	<0.150	0.193	<0.150	0.191	<0.150
hydrogencarbonate (HCO3-)	mg/L	42.3	73.2	58.5	55.2	40.8	27	26.4	65.7
carbon dioxide, total	mg/L	40	67.5	58.9	45	37.9	19.5	27.5	48.2
acidity, pH 4.5	mmol/L	<0.150	<0.150	<0.150	<0.150	<0.150	<0.150	<0.150	<0.150
carbon dioxide, free	mg/L	0.0	0.0	0.0	5.19	8.49	0.0	8.4	0.0
aggressiive carbon dioxide	mg/L	0.0	0.0	0.0	4.86	8.24	0.0	8.31	0.0
hydrogen sulphide	mg/L	53.9	40.4	7.59	18.3	3.2	<0.010	0.044	0.017
sulphide (S2-)	mg/L	50.8	38	7.14	17.2	3.01	<0.010	0.041	0.016
S, all	mg/L	206	201	184	189	188	210	189	404
Cu, all (note: unit)	µg/L	<0.0100	6.6	33.2	3.4	7.9	240	1380	<1.0
Soluble metals:									
B	mg/L	2.43	2.25	2.36	7.89	10.9	1.36	9.26	0.303
Ca	mg/L	249	267	264	257	267	252	248	450
Cu	mg/L	<0.0500	<0.0100	<0.0100	<0.050	<0.010	0.0566	0.0814	<0.0100
K	mg/L	54.7	56.1	55.1	55.2	56.9	53.7	53.6	114
Mg	mg/L	86.9	89	85.2	85	82.6	98.3	93.8	135
Mn	mg/L	0.00695	0.00801	0.00443	0.0221	0.0241	0.203	0.0763	0.0278
Na	mg/L	9380	3050	8870	3120	8970	9370	9250	9480
Si	mg/L	4.19	2.96	3.85	32.9	35.6	3.55	38.5	5.8

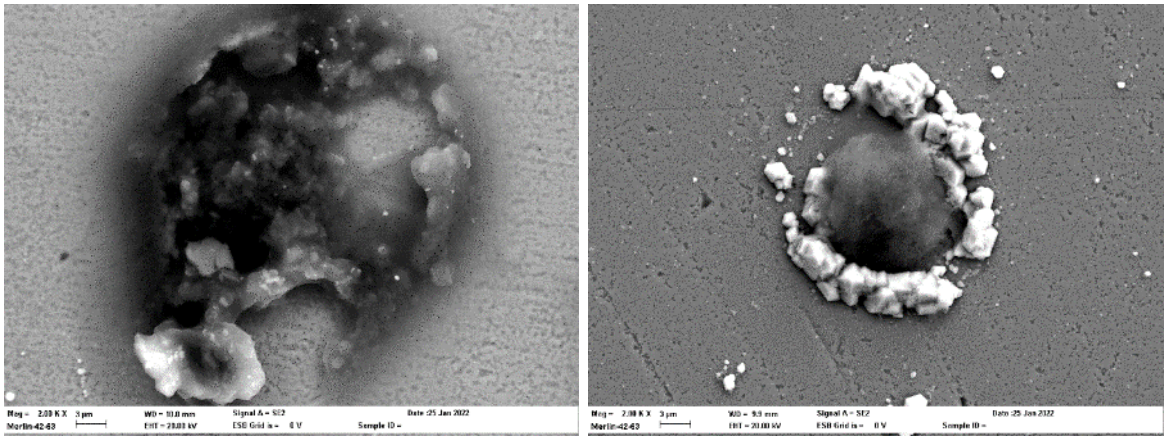
4.3 Surface characterisation with SEM

4.3.1 General observations

The characterisation of the specimens from COCOS2 and COCOS3 tests was conducted by SEM. As seen in Table 4, Table 5 and Figure 8, the surfaces were rather heterogeneous in their appearance. The surfaces did not appear to have thick uniform corrosion films on them. However, there were a few types of typical surface features in the exposed samples, which are listed in the following along with example images of the features.

(i) Figure 9: Deposits in the form of spots that could be seen as lower contrast areas in the SEM images, indicating that their average element number was lower than that of the surroundings – often due to higher content of carbon and oxygen. These deposits varied in size and shape. Even though the samples were washed in

acetone and ethanol, the setup has not been aseptic and thus the possibility of biological contamination cannot be ruled out.



a) b)

Figure 9. a) Deposits on the surface of specimen from C3-1 bottle, and thus had been exposed to 32 mg/L of sulphide with added chloride; b) deposit on the surface of specimen from bottle C3-2, where the specimens were exposed to 32 mg/L of sulphide and HCO_3^- addition.

(ii) Figure 10: Porosity, seen as areas with small holes in the mainly metallic areas. Often these holes were rather evenly distributed.

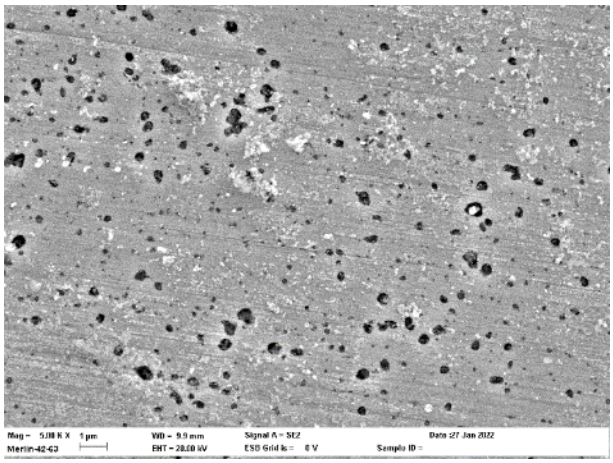


Figure 10. Porosity seen on the surface of specimen from bottle C3-4 with 32 mg/L sulphide addition at 60 °C testing temperature.

(iii) Figure 11: Clusters of larger crystals. The size of the crystals ranged from submicron to clusters of more than 10 µm in size.

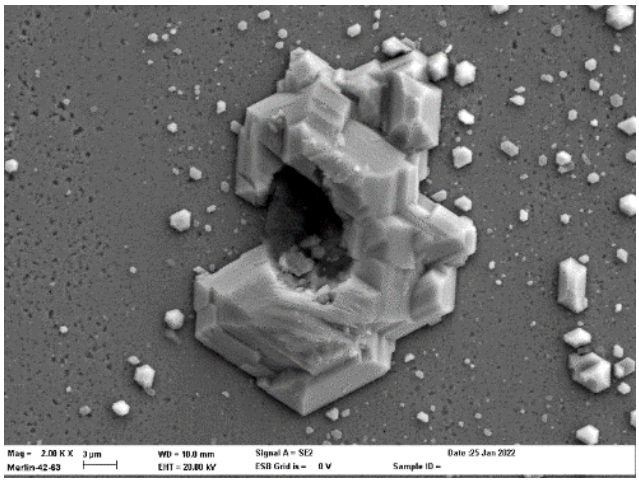


Figure 11. A crystal cluster on the surface of specimen from bottle C3-2, where the specimens were exposed to 32 mg/L of sulphide and HCO_3^- addition.

(iv) Figure 12: Small crystals on the surface, often rather evenly distributed.

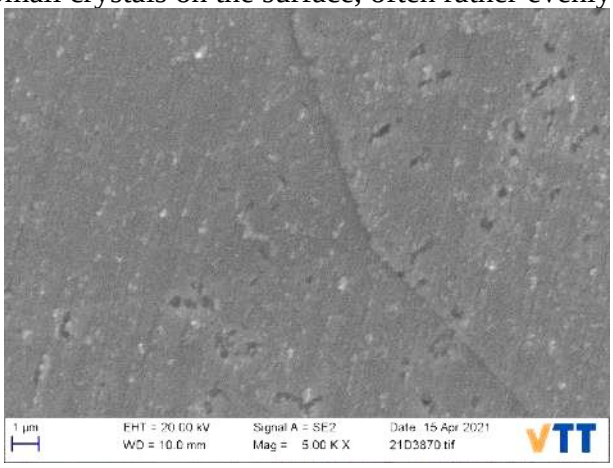


Figure 12. Small crystals on the surface of pre-oxidised specimen, which was exposed to simulated groundwater with no added sulphide in test bottle C2-1**.**

(v) Figure 13: Grain orientation-affected deposit growth, where the growth of the crystals at certain locations seems to be affected by different grains and their orientation. This is consistent with the variation in surface energy between the orientations.

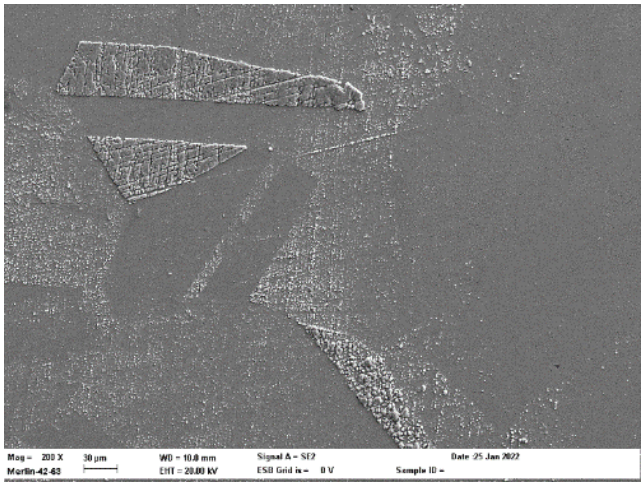


Figure 13. Grain orientation affected crystal growth on the surface of specimen from bottle C3-2, where the specimens were exposed to 32 mg/L of sulphide and HCO_3^- addition.

(vi) Figure 14: Grain orientation-affected corrosion, where the surface seems to be attacked to different extents based on the grain structure and the orientation of the grains. This feature is linked to the grain orientation affected crystal growth, but with the difference of there being no substantial crystal growth in this feature.

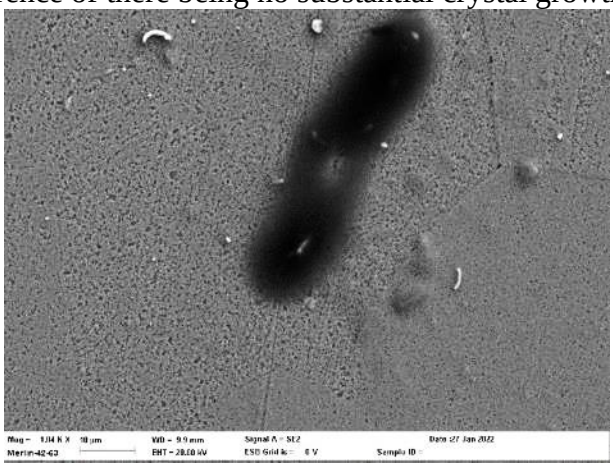


Figure 14. Grain orientation affected crystal growth on the surface of specimen from bottle C3-5, where the specimens were exposed to 32 mg/L of sulphide and chloride addition at 60 °C.

(vii) Figure 15: Attacked areas, where localised corrosion could be seen.

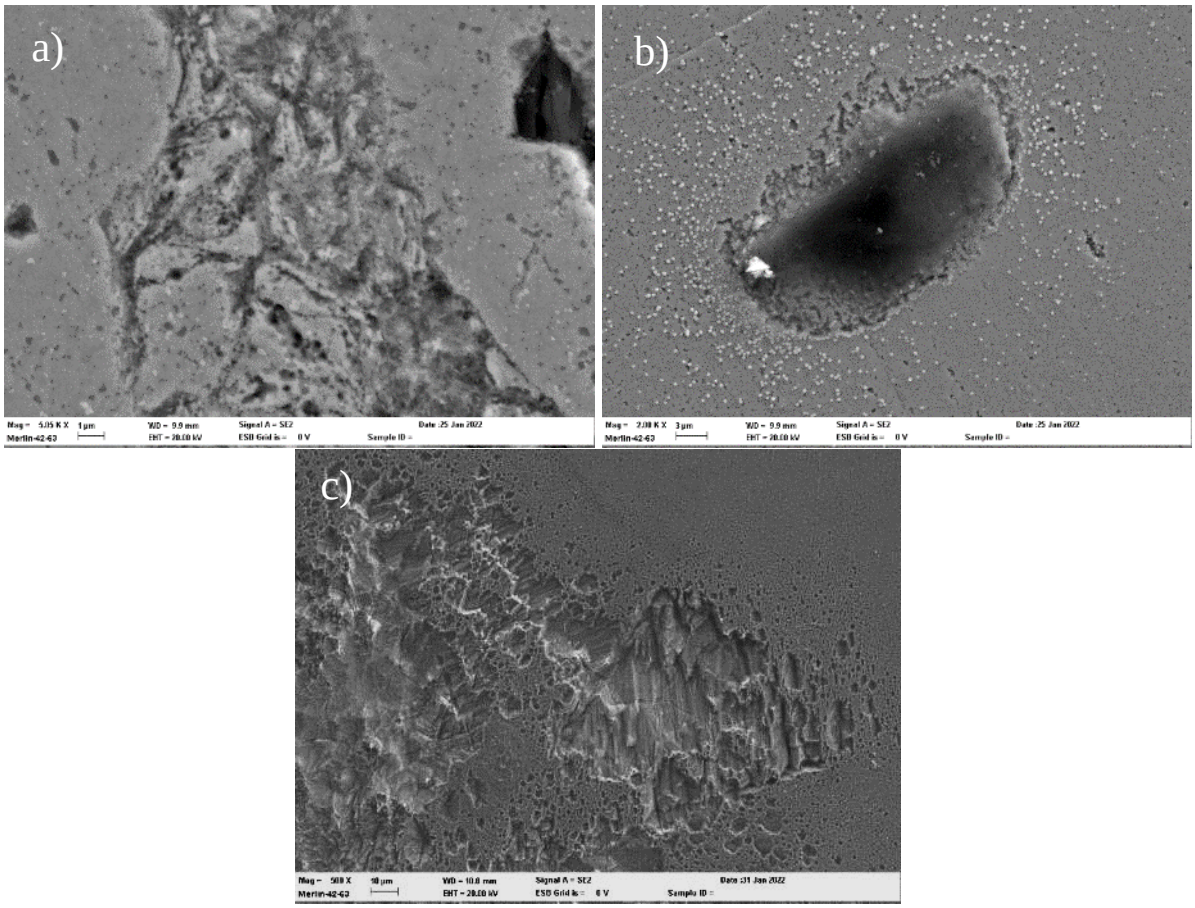


Figure 15. a) Attacked area on the surface of specimen from bottle C3-2, where the specimens were exposed to 32 mg/L of sulphide and HCO_3^- addition; b) attacked area on the surface of specimen from bottle C3-2, where the specimens were exposed to 32 mg/L of sulphide and HCO_3^- addition; c) attacked area on the surface of specimen from bottle C3-NB, where the specimens were exposed to 32 mg/L of sulphide, added chloride and bentonite.

(viii) Figure 16: Mechanically damaged areas, where the mechanical damage may have influenced the corrosion locally.

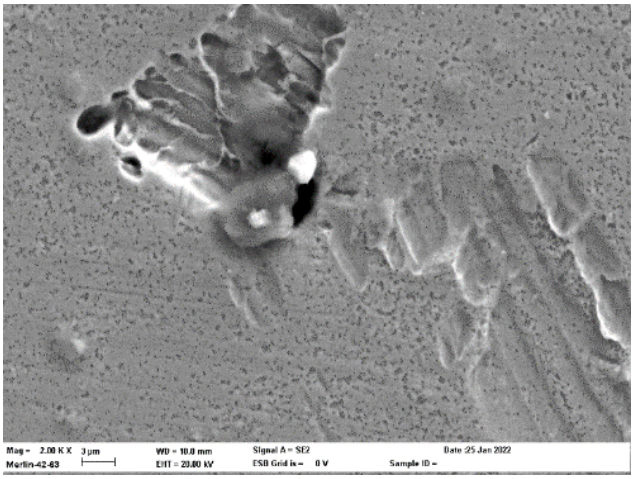


Figure 16. Seemingly mechanically damaged areas on the surface of C2-6 specimen from C3-1 bottle, and thus had been exposed to 32 mg/L of sulphide with added chloride.

(ix) Figure 17: Triangular dents and holes, which often had Si-rich material in them, possibly associated with SiC from the surface preparation with SiC grinding papers.

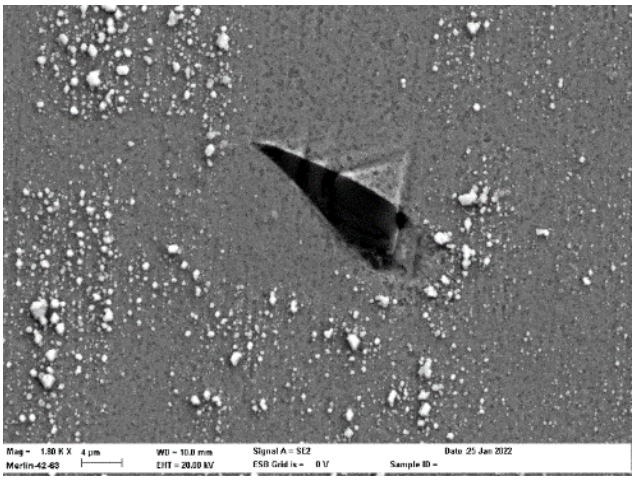


Figure 17. Triangular dent with Si-rich material on the surface of specimen from bottle C3-2, where the specimens were exposed to 32 mg/L of sulphide and HCO_3^- addition.

4.3.2 Observations from COCOS 2

In the examined COCOS2 samples, there were affected areas with porosity seen, as well as revealing of grain boundaries in some of the samples (Figure 18). There were also crystals, clustered small crystals and deposits varyingly on the surfaces.

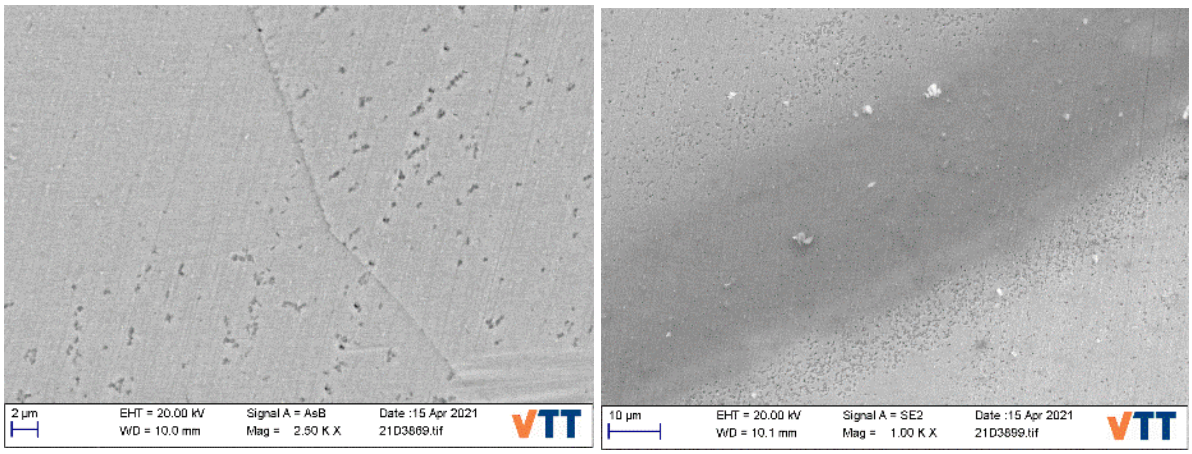


Figure 18. SEM images of a pre-oxidised sample in environment with no sulphide addition in COCOS2.

Overall, the grain orientation-dependent features were present mainly for the samples exposed to waters with no sulphide addition. This is in line with the water analyses (presented in Table 6), which show higher amount of soluble Cu after the exposure in the water with no sulphide addition.

Another observed trend was that in the samples with the highest mass loss (the ones exposed to waters containing 3.2 and 320 mg/L of sulphide, as presented in Figure 6) had the least amount of low-contrast deposits, as described as feature type (i) in section 4.3.1. This observation of difference correlates to the measurements, but the reasons behind it are unknown. On the other hand, in the samples exposed to the environments with the highest sulphide content (320 mg/L, Figure 19), there was quite a bit of crystalline deposits on the surfaces. In some cases, they were rich in Ca. Other deposits were rich in Mg and Si, raising the question about the interactions with the glass bottle, or if some Si-rich compounds are being formed aided by the water chemistry, as the amount of soluble Si in the water was the lowest in this water after the test, as shown in Table 6.

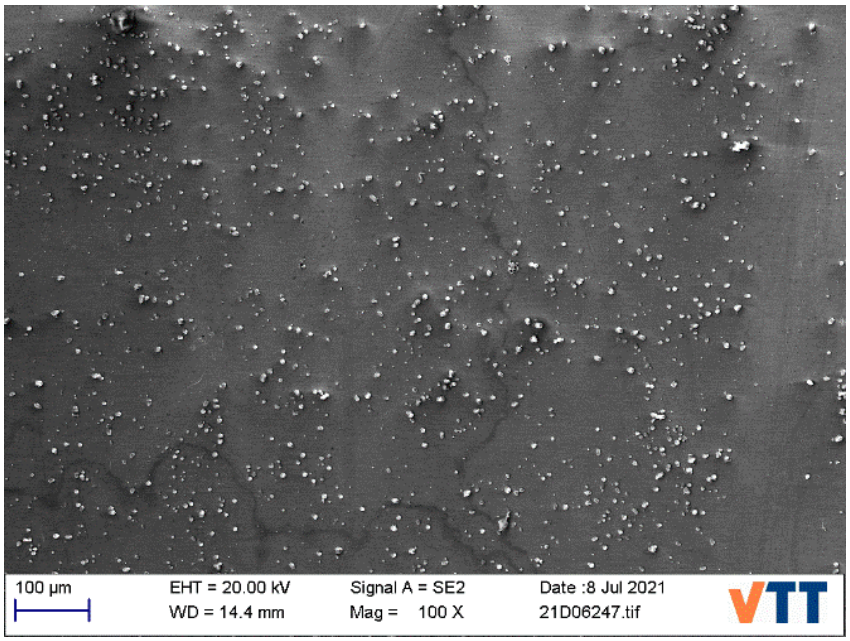


Figure 19. SEM image of a pre-oxidised sample in environment with 320 mg/L sulphide addition in COCOS2.

4.3.3 Observations from COCOS 3

In the examined COCOS3 samples, porosity, triangular dents, smudge deposits and crystals could be seen to a certain extent in practically all of the samples. The general EDS analyses of the areas revealed the sulphur content to vary between 0 and 4 atomic percent (at%) in the studied surface areas. Some clear differences could be seen in the prominence of the orientation related phenomena: grain orientation following deposit growth was visible on the selected grains in the samples which had been exposed to waters with HCO_3^- addition. Similarly, grain orientation dependent corrosion was found on the samples exposed to the elevated temperature of 60 °C. Interestingly, this was also seen on the reference samples, which had been exposed to the simulated groundwater with only added Cl^- (no sulphide addition) at both room temperature and 60 °C, as well as the sample exposed to water with added Cl^- and bentonite at room temperature.

In the formed deposits, the large crystals had a Cu/S ratio of about 2, based on EDS. The amount of oxygen in the large crystals was low, if any was detected, but carbon was often heavily present (from about 15 at% to 50 at%). The size of the crystals ranged from submicron to a few microns, and when clustered, formations of 10-20 µm could be seen. The used acceleration voltage for the EDS analyses was 20 kV, and it must be noted that some information is essentially collected underneath the surface (from the bulk material) in all of the measurements. Especially the small crystals were challenging to analyse accurately, as their size was so small that the information inevitably came from the surrounding area. Typically, they had (in addition to Cu, C and O) only < 1at% anything else.

The composition of the darker contrast deposits varied, typically having even more than 50 at% C and about 10 at% O. Also the amount of sulphur varied substantially. It must be noted that the thickness of these deposits is not known and information from the base material (copper) may also be seen in the analyses. At times, the deposits included Na-, Si-, Mg- and Cl.

4.3.4 Generalised observations made through comparisons between samples exposed to environments across COCOS2 and COCOS3

<u>Effect of preoxidation</u>

There was a slightly higher tendency in the presence of pores on the metal surfaces of the preoxidised samples than in the ground samples. On the other hand, deposit formation with distinct individual crystals on the surfaces was more prominent in the ground samples and featured both small crystal as well as larger crystal cluster formations. However, it must be noted that there was crystal formation in the deposits formed on both type samples.

<u>Sulphide content</u>

The higher sulphide content in the water manifested itself as somewhat higher amount of crystal clusters as well as small crystals on the surfaces. Higher sulphide content also correlated to a slightly higher amount of dark shallow spots, which correlated to higher amount of carbon in the area. Interestingly, the samples exposed to waters with no sulphide addition seemed to have more crystal orientation related corrosion, meaning that the amount of porosity could be linked with the orientation of the crystals.

<u>Chloride addition</u>

There was no significant systematic difference induced by the amount of Cl^- addition. Surprisingly it seemed like there were a bit more attacked areas in the samples having been

exposed to water containing the normal amount of Cl^- in the simulated water (0.149 mol/L in comparison with samples exposed to the same conditions but with additional Cl^- added (total 0.42 mol/L). However, these areas may be associated with the mechanical damage caused by handling of the samples prior to their exposure.

Hydrogen carbonate addition

The addition of HCO_3^- (total amount of 0.0007 mol/L) seemed to have a rather clear effect on the appearance of the sample surfaces. The samples exposed to water without the HCO_3^- addition (total amount of 0.0002 mol/L) had more dark shallow spots. In turn, the samples exposed to water with the same chemistry but with added HCO_3^- had more grain orientation following deposit growth with distinct crystals in the surface, meaning that the amount of crystals seemed to be dependent on the orientation of the grain.

Effect of temperature

Comparing the sample surfaces between the samples in the same water chemistry but at the temperature of 22 or 60 °C, it seemed that there were more crystal clusters and grain orientation affected corrosion at 60 °C. This could mean that any differences in kinetics influenced by orientation were accelerated and thus highlighted by the raise in the temperature.

4.4 EBSD for cross-sectional samples (COCOS2)

The electron backscatter diffraction (EBSD) investigations were conducted for four samples from COCOS2 test:
1) no pre-oxidation, no sulphide (C2-1-n), 2) pre-oxidation, no sulphide (C2-1-o), 3) no pre-oxidation, 32 mg sulphide (C2-3-n), and 4) pre-oxidation, 32 mg sulphide (C2-3-o).

The results from the EBSD investigations are shown in Figures 20-23. They revealed that pre-oxidation of the surface increased particularly the number of low-angle grain boundaries (LAGB) with <10° misorientation. In the case of test environments with no added sulphide (1, 2), the number of low-angle grain boundaries in the absence of pre-oxidation was 49812, while that in the presence of pre-oxidation was 74478. In the test environments with 32 mg/L added sulphide, the corresponding figures were 68231 (no pre-oxidation) and 171654 (with pre-oxidation), reflecting the significant contribution by pre-oxidation to the number of LAGB. In the environment with no added sulphide, also the number of high-angle grain boundaries (HAGB) with the misorientation >10° increased slightly due to the pre-oxidation of the copper surface, from 315456 (no pre-oxidation) to 372126 (with pre-oxidation). However, when the test environment was added with 32 mg/L sulphide, the number of HAGB was decreased from 329968 (no pre-oxidation) to 234946 (with pre-oxidation). The observations about the Grain Average Misorientation (GAM) maps disclosed only small grain average misorientations at the surface of the specimens for non-pre-oxidised samples (Figs. 19d and 21d) but clearly greater GAM occurrence just underneath the sample surface for pre-oxidised samples. Therefore, the obtained results suggest that pre-oxidation of the copper samples contributes to the strain localization in the near-surface areas of the samples, down to approximately 100 μm. The role of the presence of sulphide in the test environment is similarly reflected essentially to the increase in the number of LAGBs as compared to corresponding cases with no added sulphide. It is emphasized that the size of sulphur atom is larger than that of oxygen atom, therefore sulphide compounds that form on the sample surfaces likely accommodate greater volumes, creating also higher strains in the near-surface areas of the material.

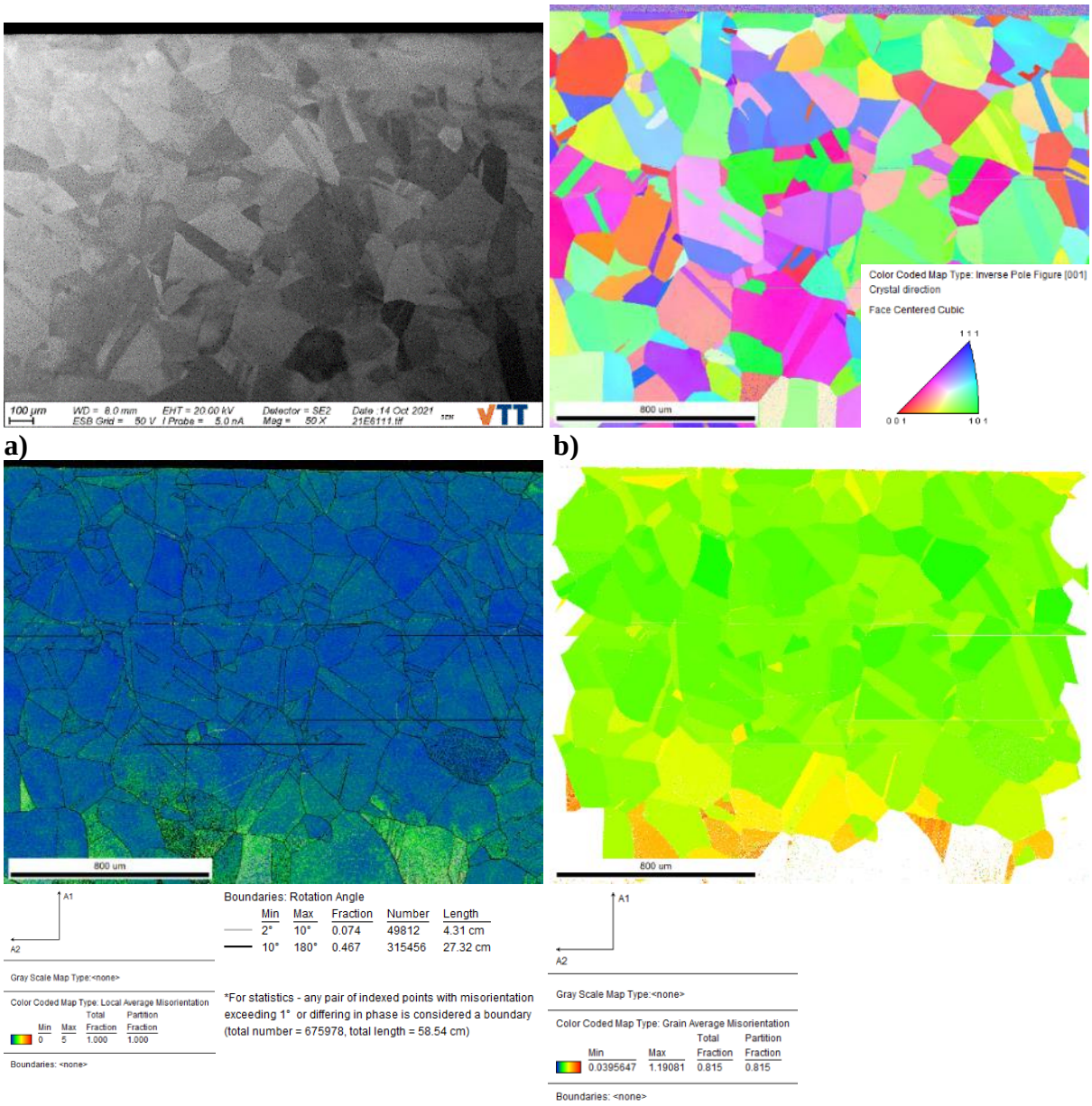


Figure 20. Results from EBSD investigations conducted for cross-section of the specimen (C2-1-n, no pre-oxidation, 0 mg/L S environment). a) SE image of the examined area. b) IPF showing the orientation of the grains. c) LAM map showing the misorientation of the grains. d) GAM map.

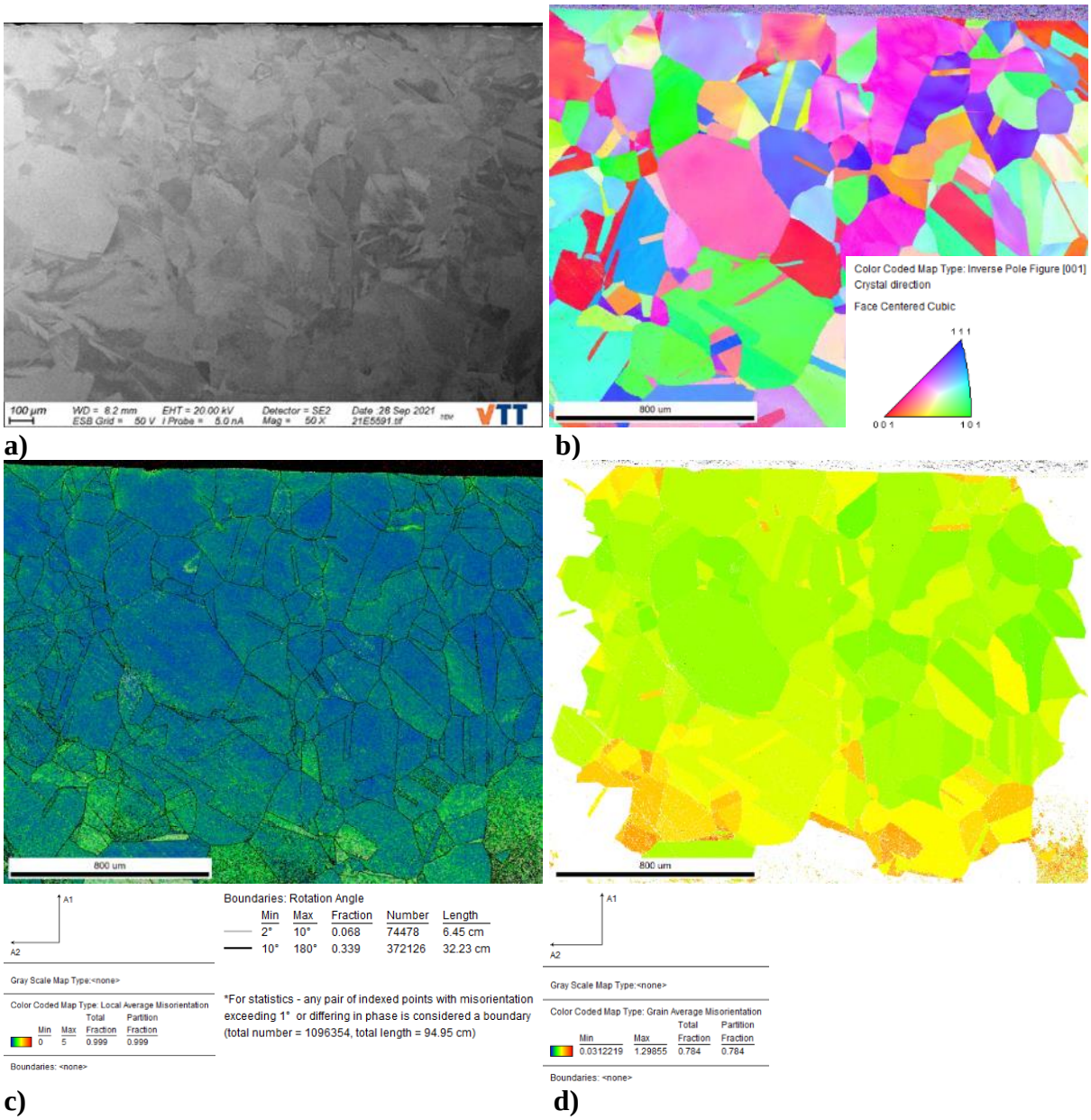


Figure 21. Results from EBSD investigations conducted for cross-section of the specimen (C2-1-o, pre-oxidated, 0 mg/L S environment). a) SE image of the examined area. b) IPF showing the orientation of the grains. c) LAM map showing the misorientation of the grains. d) GAM map.

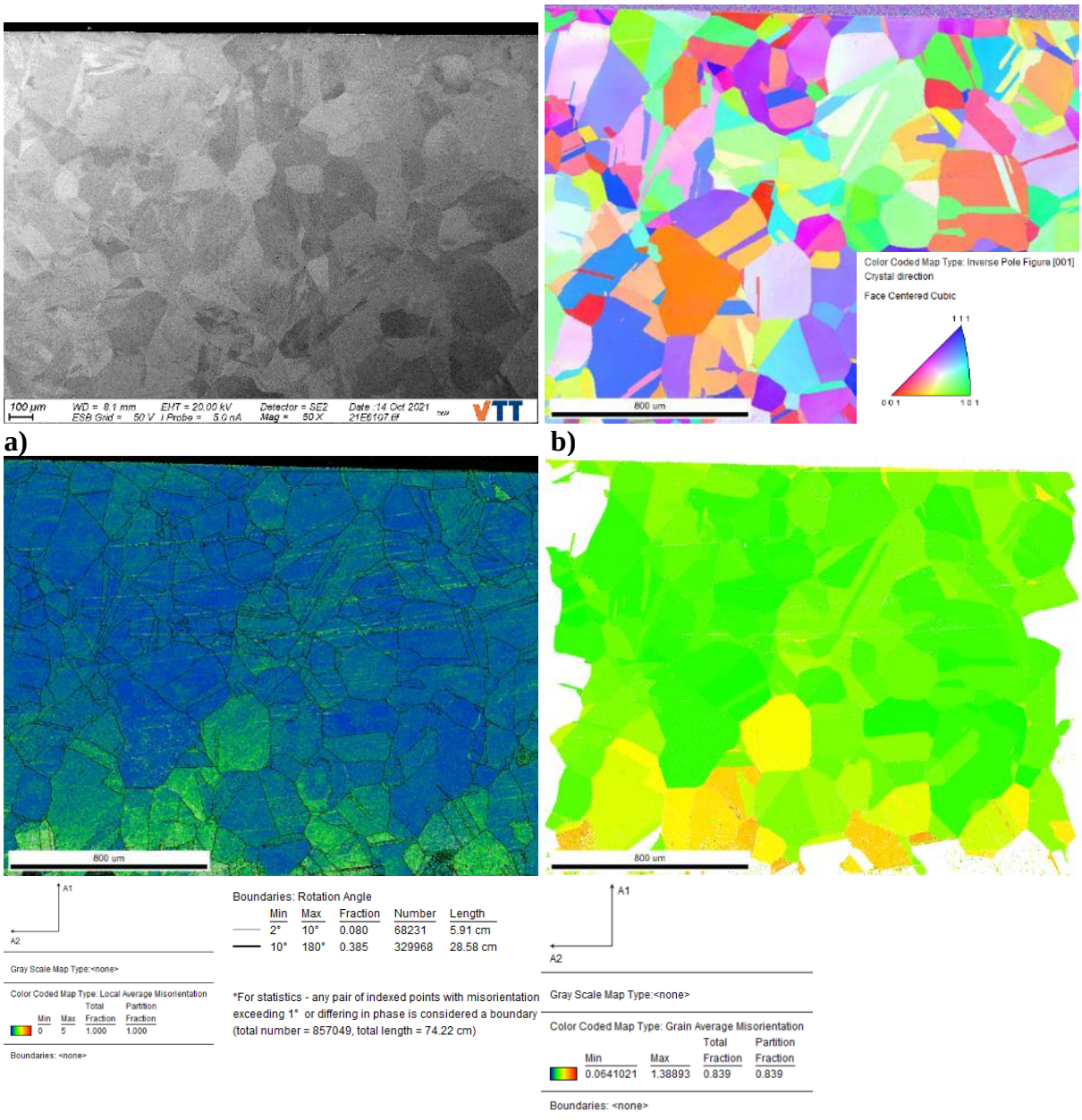


Figure 22. Results from EBSD investigations conducted for cross-section of the specimen (C2-3-n, no pre-oxidation, 32 mg/L S environment). a) SE image of the examined area. b) IPF showing the orientation of the grains. c) LAM map showing the misorientation of the grains. d) GAM map**.**

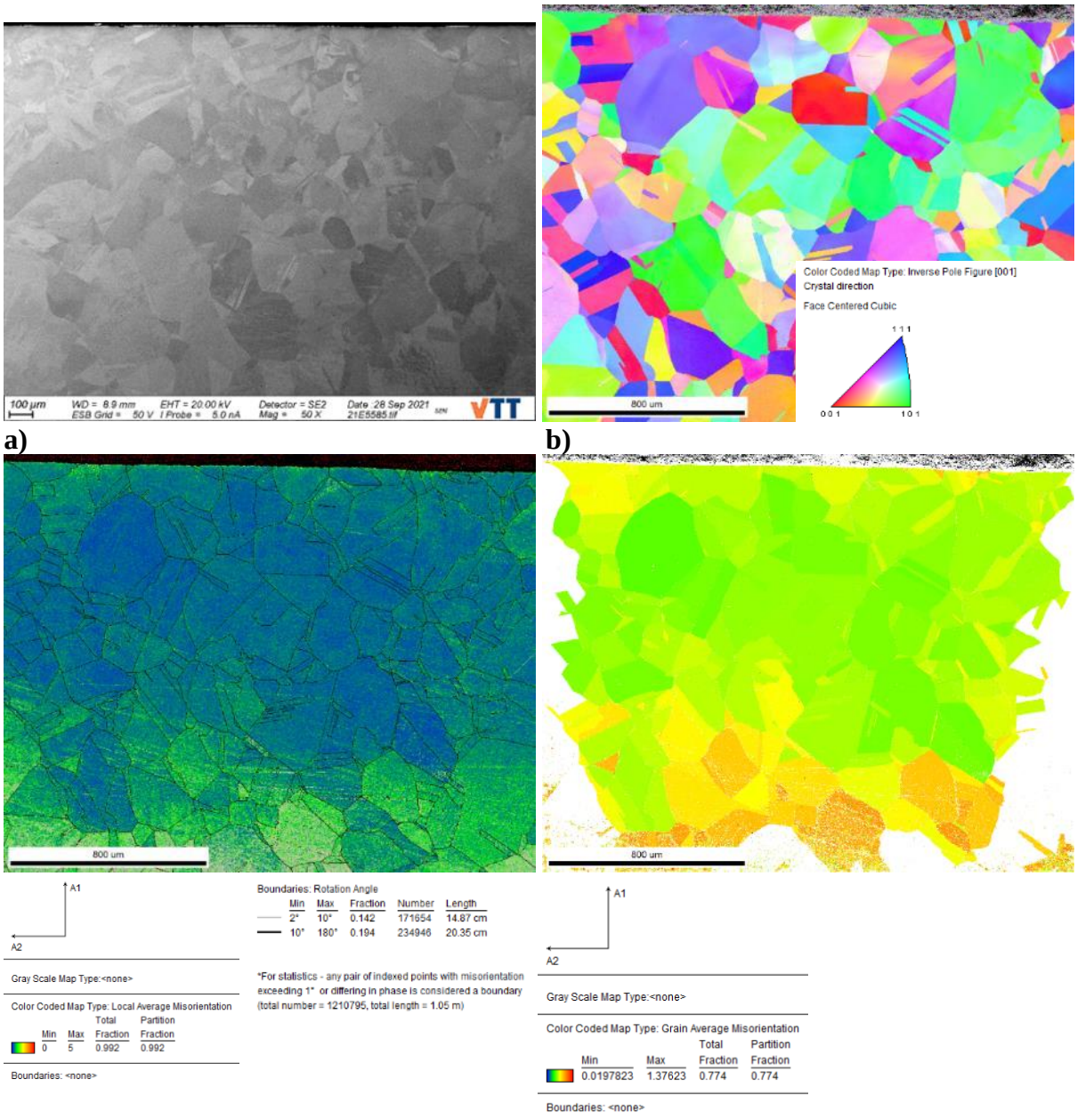


Figure 23. Results from EBSD investigations conducted for cross-section of the specimen (C2-3-o, pre-oxidated, 32 mg/L S environment). a) SE image of the examined area. b) IPF showing the orientation of the grains. c) LAM map showing the misorientation of the grains. d) GAM map.

4.5 GDOES

Glow Discharge Optical Emission Spectroscopy (GDOES) analysis was performed to study the location of key elements: sulphur and oxygen, in the near-surface areas of the samples, mainly because of their tendency to participate in the deposit formation. Figures 25-26 show the detected levelts of oxygen and sulphur in two COCOS2 samples that were exposed to 32 mg/L sulpide environment for 9 months (bottle C2-3). X-axis shows the depth from the surface. Here, the results are shown only for the first micrometer depth. Two spots for both samples were measured. For ground sample (no pre-oxidation) the results are shown in Figure 24. In the surface layer, the sulphur concentration in first measurement spot was 25 mass-% and the respective oxygen concentration was 12 %, whereas in another spot the corresponding values

were 43 % and 30 %. These results imply that the outermost areas of the deposit was essentially enriched in sulphur, yet oxygen was also involved. The thickness of the sulphur- and oxygen-bearing surface film was approximately 2-4 nm, i.e., in the same range as typical passive films. However, the concentration of oxygen levelled to constant only in the depth of about 10-40 nm. This may be linked with grinding of the surfaces, hence the presence os surface roughness. At the depth of approximately 240 nm, a peak in S and O contents in the second measurement spot could be detected. This may be due to, e.g., the contribution by grain boundaries just underneath the surface (from the neighbouring grains etc).Due to the thinness of the overall surface film and the fact that the test conditions were oxic, it is possible that the oxygen was included in the surface priot to tests, i.e., after the grinding procedure.

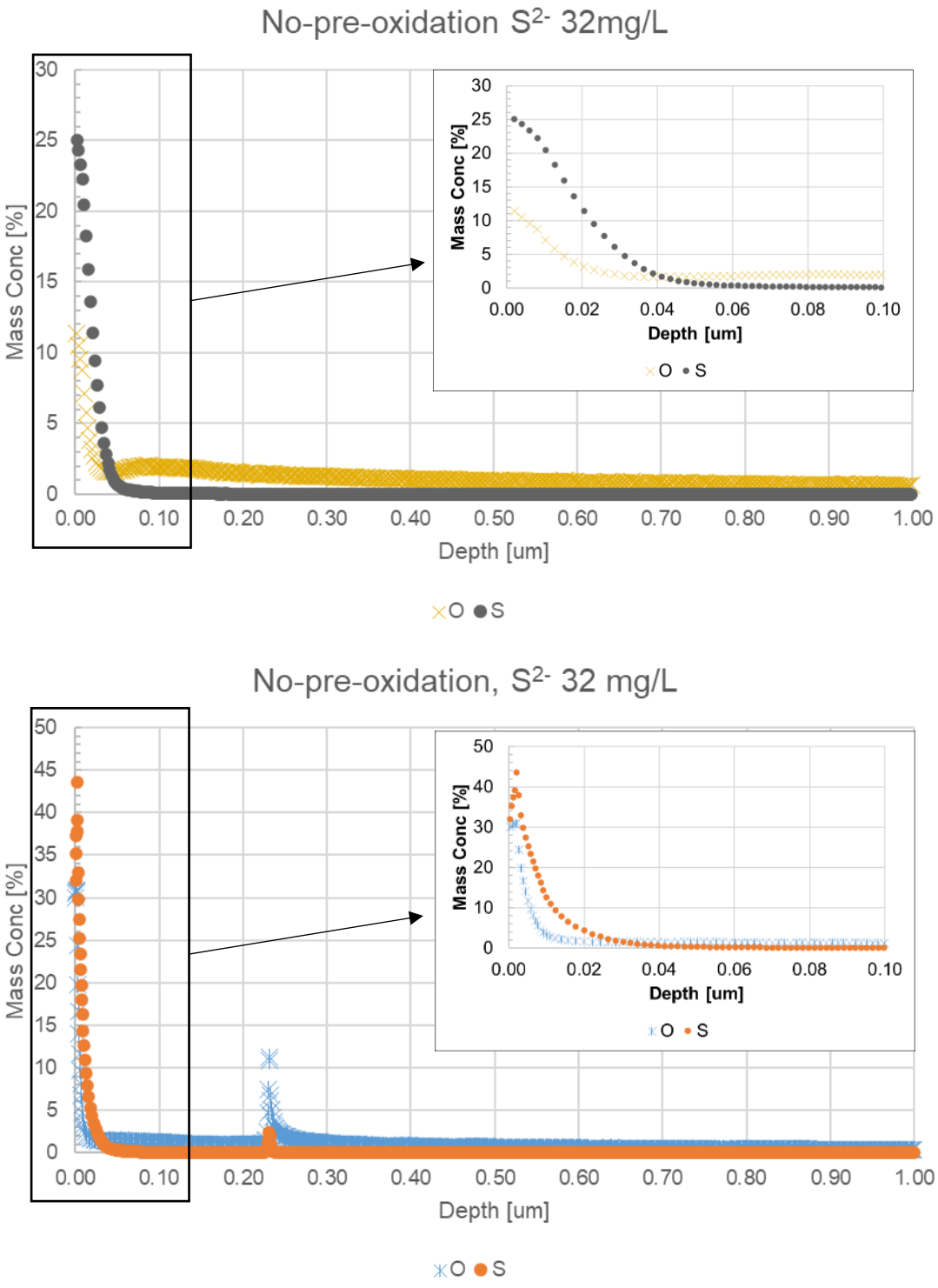


Figure 24. Mass concentration depth profile for oxygen and sulphur in non-pre-oxidised sample (ground) exposed to 32 mg/L S environment (C2-3) by GDOES, two spots from one sample measured.

Figure 25 shows two GDOES depth profiles measured on two spots on pre-oxidazed sample. Here, the depth profiles for S and O concentrations close to the surface were evidently different compared to the sample that was not pre-oxidized. First, the relative S and O concentrations at the maximum level were almost equal, indicating that the oxide film which was formed before the tests was partly retained at the surfaces despite the contribution of S. Second, as compared

to the ground surface (Fig. 25), the surface film was thicker, approximately 12-15 nm. However, increased levels of oxygen were detected down to the level of about 45 nm below the surface, likely due to the surface roughness produced by gringing and following pre-oxidation.

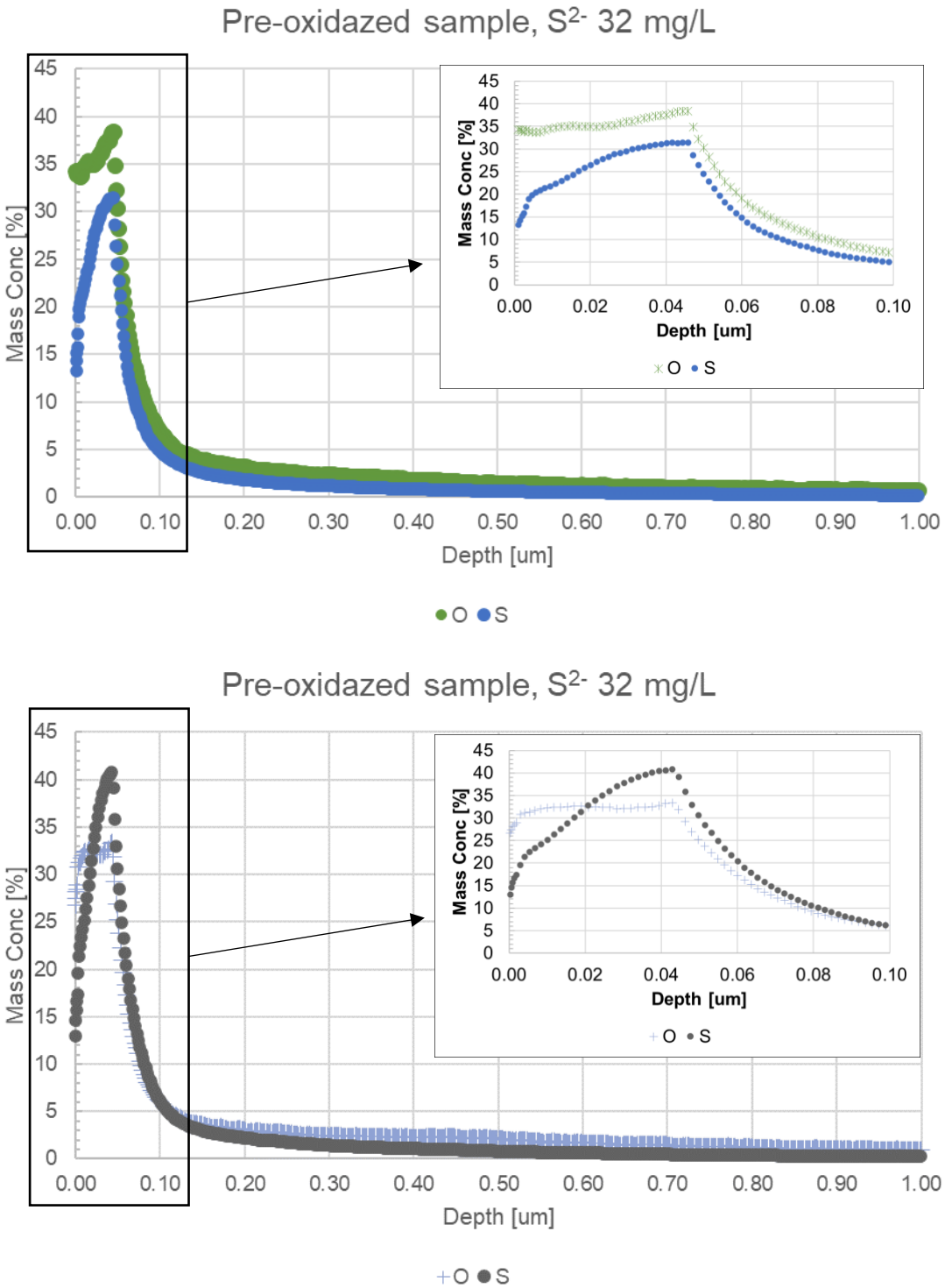


Figure 25. Mass concentration depth profile for oxygen and sulphur in pre-oxidised sample exposed to 32 mg/L S environment (C2-3) by GDOES, two spots from one sample measured.

4.6 Synchrotron GIXRD results

A brief summary of the synchrotron GIXRD results, mainly the identification of crystalline corrosion products, was included in the previous annual report. Moreover, the results also show the structure changes occurred in the copper lattice due to the exposure. From the lattice parameter calculated in and out of the sample surface plane for the two incidence angles, the unit cell volume and relative strain could be calculated. The sulphide-induced structure changes are more pronounced in the region near the surface, as judged from the data at different incidence angles. In general, the content of sulphide has an influence on the structure changes, but there is no a simple linear relationship. There is also an inhomogeneous distortion of the unit cell, indicated by the relative strain in- and out-of-plane.

Detailed data analysis and key findings will be published at a peer-reviewed scientific journal.

4.7 Synchrotron HEXRD results

In general, the High energy X-ray diffraction (HEXRD) results indicate heterogeneous lattice deformation of the exposed copper samples. Key findings from the first three samples, combined with density functional theory calculations, were reported in a peer-reviewed paper published at *Corrosion Science* (**184** (2021) 109390). SKB raised some comments on our paper, and we have replied the comments with detailed explanations and emphasized the need for further studies using advanced techniques. Both the comments and the replies are published at *Corrosion Science* (199 (2022) 110182, and 199 (2022) 110183). Detailed data analysis of the recent measurements is ongoing, and the findings will be published later at some peer-reviewed scientific journal.

4.8 ToF-SIMS results

Being one of further studies of copper corrosion caused by sulfide-containing ground water, recently we performed Time-of-Flight Secondary Ion Mass Spectroscopy (ToF-SIMS) analysis of the exposed copper samples. The ToF-SIMS results are very interesting, providing detailed information of the penetration of the corrosive species, S, Cl, O and H, into the copper microstructure, which is not uniform and clearly related to the microstructure. The per-oxidation, exposure time, added Na_2S, as well as the temperature, all have an influence on the corrosion penetration. The temperature has the most pronounced effect, and increasing from 20 to 60 °C led to more than 10 times increase of the penetration depth of the corrosive species. An example of the results is shown in the figure below, including in-depth elemental profiles, 2D mapping of the distribution of the corrosive species, and a 3D presentation of the corrosive species (or corrosion products) heterogeneously distributed in the copper microstructure. The ToF-SIMS results also revealed the influence of grain orientation corrosion as judged by the penetration of the corrosive species, Figure 26.

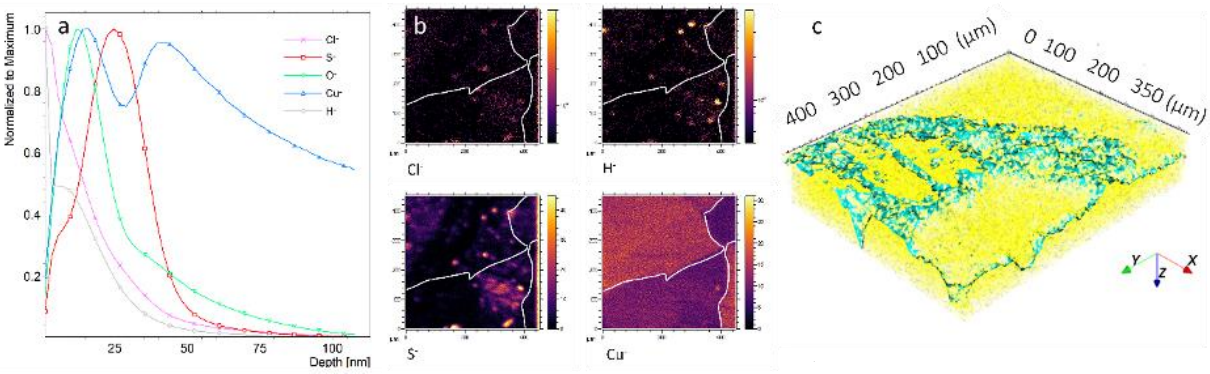


Figure 26. (a) SIMS Depth profiles through the first 100 nm oxide layer on a Cu-OFP copper sample exposed to ground water with 0.001M Na_2S for 9 months, showing a substantial penetration of S through the oxide layer and into the bulk Cu. (b) ToF-SIMS 2D images of the Cu microstructure at 40 nm depth from the sample in (a), showing the Cl-(log), H-(log), S- and Cu- signals. White lines indicate grain boundaries. (c) A 3D SIMS data from a Cu-OFP sample exposed to ground water with 0.001M Na_2S for 4 months reveals penetration of S along the grain boundaries.

The key results of ToF-SIMS were presented at the 18th Nordic Corrosion Congress, May 31-June 2, 2022, Turku, Finland. A manuscript is under preparation for publication at a peer-reviewed scientific journal.

5. Discussion

The role of sulphide containing environment in the corrosion performance of copper is complex. Based on this study, the sulphide content and corrosion rate of copper are not directly proportional. In some of the tests, electrochemical measurements disclosed sharp changes in open circuit potential that could be linked with oxygen reactions. However, in such cases where the open circuit potential values were retained constant all through the test, the samples were situated at highly negative potential levels typical of copper sulphide formation. The corrosion rates determined with electrochemical measurements revealed low corrosion rates of less than 5 µm/a. The lowest values were typically detected in such cases, where the open circuit potential was constant and low. Mass loss based cumulative corrosion rate determination disclosed corrosion rates of the magnitude of 0.5 µm/a or less for the samples tested at room temperature without sulphide addition or sulphide addition of 32 mg/L. The corrosion rates of copper in 32 mg/L sulphide environment increased in the tests conducted at the temperature of 60 ºC, so that the cumulative corrosion rate of copper was 1.3 µm/a. The samples exposed for 9 months to 3.2 mg/L and 320 mg/L sulphide resulted in corrosion rate values above 10 µm/a.

The findings in sample characterisations showed differences in copper samples exposed to environments with different sulphide contents. In visual inspection, already the colour of surfaces varied between the sulphide levels. SEM characterisations revealed a few types of typical surface features in the exposed samples, which were rather heterogeneous for their surface appearances. The exposure to the simulated groundwater with higher amount of sulphide could be generally seen as a higher amount of crystal formation on the surfaces. The samples exposed to the simulated groundwater with no sulphide addition showed stronger dependency between the porosity and grain orientation.

Amount of Cl^- and HCO_3^- and their effects were already discussed in first yearly report of COCOS project (Ratia et al., 2020). King and Lilja (2014)conclude based on collecting several different references the most important ion species regarding the pitting of copper are Cl^-, SO_4^{2-} and HCO_3^-: increasing amount of HCO_3^- promotes passivation, whereas Cl^- and SO_4^{2-} are promoting the breakdown of the film. In this study, the highest interest was on studying the effects of sulphide concentrations, but also different ratios of Cl^- and HCO_3^- were added to test solution to study the effect on corrosion behaviour. Electrochemical measurements or mass loss-based corrosion rate determinations did not show significant differences between the copper behaviour in solutions with different Cl^- and HCO_3^- concentrations with constant sulphide concentration of 32 mg/L. In simulated groundwater without sulphide addition but with added chloride, the dissolution of copper was higher based on water analyses, indicating that in the presence of chloride, sulphide addition provides protection for the dissolution of copper. This was due to enhanced deposit formation. In SEM studies, it was noted that the samples exposed to water with added HCO_3^- had more grain orientation following deposit growth with distinct crystals in the surface. Indeed, water chemistry is important and it is noted that in this study, the change in pH with added sulphide or hydrogen carbonate was not compensated. Similar measurements and studies of ion species could be conducted in future using solution that could act as pH buffer.

GDOES results that were obtained for ground COCOS2 samples subjected to simulated groundwater with 32 mg/L sulphide addition featured a typical thickness of passive films, 2-4 nm. The film was essentially rich in S, consistently with the OCP values that are typical for copper sulphide formation, yet it also involved some O, which may originate from natural air-formed oxide film that may have formed between grinding of the samples and their exposure

to the anoxic test solutions. The results also revealed that when pre-oxidation of the samples is used in sample preparation, the resulting surface films are somewhat thicker, approximately 12-15 nm, thus not perfect passive films in their thickness. Also compositionally they contained relatively equal amounts of O and S. The work done with ToF-SIMS studies continues detailed studies of the penetration of the corrosive species, S, Cl, O and H, into the copper microstructure.

In general, creating corrosion tests to simulate long-term behaviour in repository scale acquires always acceptance of the extrapolation of results and making assumptions on the long-term behaviour of similar systems. It is noted that the duration of the test varied in COCOS between the test campaigns, which may have an effect on the corrosion rate determination based on mass loss as corrosion processes are not linear. However, when comparing the findings from 2 to 9 month long tests, no phenomenological differences in corrosion mechanisms were found, although unexpected differences between mass losses were recorded. In case of electrochemical measurements, stabilization in potential occurs after around 100 days of experiment. In that sense, the 4 month long electrochemical tests are considered as reliable as the 9 month tests. Moreover, technical challenges with experimental equipment were found during this project related to the oxygen leakages in test bottles and corrosion of glass vessels when using high sulphide concentrations, that was reported in previous annual reports.

The advanced material characterisation methods provided insightful information about the copper microstructure and effect of long-time immersion in sulphide containing water. EBSD results suggested that both the pre-oxidation treatment and the exposure to sulphide environment introduced the strain localization in the near-surface areas of samples. GIXRD and HEXRD results showed significant heterogeneous structure deformation in the copper lattice due to the exposure, both in the near surface region and deep inside the copper microstructure. Moreover, ToF-SIMS measurement provided in-depth and lateral distribution of the corrosive species, S, Cl, O and H penetrated into the copper matrix, and the results reveal the preferential ingress of the corrosive species via grain boundaries. In all the exposed copper samples, S, O, Cl, and H were detected, heterogeneously distributed in the microstructure, the amount and depth are influenced by the level of added sulfide, the temperature of groundwater, and the existence of initial oxide film. Temperature has the strongest effect. Surprisingly, not only S and H, but also Cl and O, have penetrated quite deeply into the copper microstructure. Nano-SIMS with nanometer resolution is needed to map H distribution along grain boundaries.

The results from these analyses of the exposure-induced copper corrosion using the advanced analytical techniques demonstrated that the corrosion not only occurs on the surface, corrosive species such as S, Cl, O and H can penetrate deeply into the copper microstructure via defects such as grain boundaries, and lead to local degradation of the microstructure. Further studies are needed to achieve a fundamental understanding of the mechanisms for the corrosion penetration and their consequences regarding, e.g., embrittlement and cracking, which is still missing in the scientific basis for the risk assessment for the final disposal of nuclear waste.

6. Conclusions

The corrosion behaviour of OFP-copper in simulated environment with the water chemistry near groundwater with sulphide additions was studied in NKS-R-COCOS project. As outcome of the project, following conclusions can be drawn:

- The sulphide-copper interactions and formation of sulphide film on copper surface are complex processes and the measurable corrosion is not proportional to sulphide concentration.

- The corrosion is not always uniform and therefore the traditional measurement methods, such as mass loss determination and linear polarisation techniques do not give clear indications of the corrosion risks. The corrosion rates acquired with these methods were 0-12.3 µm/a, depending on the sulphide concentration, temperature and other variables between tests.

- The role of oxide layer formed on the copper surface before placing the canister in repository should not be omitted. In this study, a pre-oxidation was done for copper samples to be studied in corrosion tests. The presence of oxide layer was found to affect the corrosion behaviour and e.g. the penetration of corrosive elements into the bulk copper.

More work is needed to define the nature and chemistry of the surface films that develop on copper surfaces after such reaction sequences that first involve and oxic period followed by an anoxic period. The penetration of chemical elements, namely S, H, Cl and O, should be studied to verify the integrity of copper in such environments. Modern in-depth methods of material characterisation can discover even small changes in microstructures.

Acknowledgments

NKS conveys its gratitude to all organizations and persons who by means of financial support or contributions in kind have made the work presented in this report possible.

Taru Lehtikuusi and Tuomo Kinnunen are gratefully acknowledged for their assistance with the experiments at VTT, as well as Mervi Somervuori for SEM images and EDS measurements.

We acknowledge PETRA III at DESY in Germany for providing the access to the beamline P21.2 for the synchrotron HEXRD measurement, Diamond Light Source in UK for the access to the beamline I07 for the synchrotron GIXRD measurement. Assoc. Prof. Per Malmberg at the Infrastructure for Chemical Imaging at Chalmers University of Technology is greatly acknowledged for the assistant in the ToF-SIMS measurement. Moreover, we thank the Swedish National Infrastructure for Computing (SNIC) for providing the Swedish super-computing resource that enabled the DFT calculations.

Disclaimer

The views expressed in this document remain the responsibility of the author(s) and do not necessarily reflect those of NKS. In particular, neither NKS nor any other organisation or body supporting NKS activities can be held responsible for the material presented in this report.

7. References

Hall, D. S., Behazin, M., Jeffrey Binns, W., & Keech, P. G. (2021). An evaluation of corrosion processes affecting copper-coated nuclear waste containers in a deep geological repository. *Progress in Materials Science*, *118*(April), 100766. https://doi.org/10.1016/j.pmatsci.2020.100766

Huttunen-Saarivirta, E., Ghanbari, E., Mao, F., Rajala, P., Carpén, L., & Macdonald, D. D. (2018). Kinetic Properties of the Passive Film on Copper in the Presence of Sulfate-Reducing Bacteria. *Journal of The Electrochemical Society*, *165*(9), C450–C460. https://doi.org/10.1149/2.007189jes

Huttunen-Saarivirta, E., Rajala, P., Bomberg, M., & Carpén, L. (2017). Corrosion of copper in oxygen-deficient groundwater with and without deep bedrock micro-organisms: Characterisation of microbial communities and surface processes. *Applied Surface Science*, *396*, 1044–1057. https://doi.org/10.1016/j.apsusc.2016.11.086

Isotahdon, E., Ratia, V., Rajala, P., Carpén, L., Örnek, C., Zhang, F., & Pan, J. (2021). *NKS-447, Corrosion of copper in sulphide containing environment: the role and properties of sulphide films-Annual report 2020*. www.nks.org

King, F, & Lilja, C. (2014). Localised corrosion of copper canisters. *Corrosion Engineering Science and Technology*, *49*(6), 420–424. https://doi.org/10.1179/1743278214Y.0000000182

King, Fraser, Lilja, C., Pedersen, K., & Pitkänen, P. (2012). *An update of the state of the art report on the corrosion of copper under expected conditions in a deep geologic repository*. *31*(December), 180.

Nuclear Waste State of the Art Report 2011 (p. 81). (2011). The Swedish National Council for Nuclear Waste Report.

Ratia, V., Carpén, L., Isotahdon, E., Örnek, C., Zhang, F., & Pan, J. (2020). *NKS-434, Corrosion of copper in sulphide containing environment: the role and properties of sulphide films – Annual report 2019*. www.nks.org

Salonen, T., Lamminmäki, T., King, F., & Pastina, B. (2021). Status report of the Finnish spent fuel geologic repository programme and ongoing corrosion studies. *Materials and Corrosion*, *72*(1–2), 14–24. https://doi.org/10.1002/maco.202011805

SKB. (2019). Supplementary information on canister integrity issues. In *SKB-TR-19-15* (Issue March, p. 135). SKB - Svensk Kärnbränslehantering AB. www.skb.se

Bibliographic Data Sheet **NKS-460**

Title	Corrosion of copper in sulphide containing environment: the role and properties of sulphide films – Annual report 2021
Author(s)	Elisa Isotahdon[1], Vilma Ratia[1], Elina Huttunen-Saarivirta[1], Xiaoqi Yue[2], Jinshan Pan[2]
Affiliation(s)	[1]VTT Technical Research Centre of Finland Ltd., Espoo, Finland [2]KTH Royal Institute of Technology, Stockholm, Sweden
ISBN	978-87-7893-553-3
Date	June 2022
Project	NKS-R / COCOS
No. of pages	39
No. of tables	7
No. of illustrations	26
No. of references	10

Abstract
max. 2000 characters

In NKS-R COCOS project, the role and properties of sulphide films on copper surface were studied. This is the third annual and final report of the project.

OFP-copper samples were exposed to sulfide-containing (0-640 mg/L) anoxic simulated groundwater for different durations between 2 to 9 months. A pre-oxidation procedure was used to simulate the effect of oxic period of repository to copper surface. The corrosion behaviour was studied using mass loss determination, electrochemical measurements and several modern material characterisation methods after the exposure. In addition to sulphide concentration the chemistry of test solution was varied by additions of chloride and hydrogen carbonate. Specimens and surface deposits were studied with electron microscopy (SEM+EDS, EBSD). In-depth characterisation was done using GD-OES analysis, HE-XRD techniques and SIMS analysis. During the project, also several other analysis methods were used.

The measurable corrosion was not proportional to sulphide concentration. The corrosion was not always uniform. The corrosion rates were 0-12.3 µm/a, depending on the sulphide concentration, temperature and other variables of the environment.

EBSD results suggested that both the pre-oxidation treatment and the exposure to sulphide environment introduced the strain localization in the near-surface areas of samples. HE-XRD results showed significant heterogeneous structure deformation in the copper lattice after the

exposure to test environment, both in the near surface region and deep inside the microstructure.

The sulphide-copper interactions and formation of sulphide film on copper surface were found complex processes. In this project, the world-class analytical techniques were used to investigate the penetration of chemical species into the copper microstructure. More work is needed to define the role of these chemical species as well as the nature and chemistry of the surface films that develop on copper surfaces in repository conditions.

Key words corrosion, copper, nuclear waste, sulphide